Geophysical Journal International

Geophys. J. Int. (2018) **213,** 1503–1523
Advance Access publication 2018 February 7
GJI Geomagnetism, rock magnetism and palaeomagnetism

doi: 10.1093/gji/ggy041

Does Deccan Volcanic Sequence contain more reversals than the three-Chron N–R–N flow magnetostratigraphy?—a palaeomagnetic evidence from the dyke-swarm near Mumbai

N. Basavaiah,[1] K.V.V. Satyanarayana,[1] K. Deenadayalan[1] and J.N. Prasad[2]

[1]*Indian Institute of Geomagnetism, Kalamboli, New Panvel, Navi Mumbai* 410218, *India. E-mail: bas@iigs.iigm.res.in*
[2]*Department of Physics, Ranchi University, Ranchi* 834008, *Jharkhand, India*

Accepted 2018 February 5. Received 2018 January 26; in original form 2017 May 31

SUMMARY

New palaeomagnetic data from a series of Deccan-age dykes cutting across the basement of lava flows along east and south of Mumbai (18°–19°N and 72°–73.5°E) have uncovered both normal (N) and reverse (R) magnetizations. Out of 33 dykes investigated, 29 dykes have yielded stable characteristic remanent magnetizations (ChRM) amenable for statistical analysis. Twenty dykes exhibit N-polarity and nine dykes show R-polarity. The tilt-corrected dyke virtual geomagnetic poles reveal two distinct groups of dykes. Each group consists of both N- and R-polarity dykes on the Indian apparent polar wander path (APWP). The mean of N-polarity dykes is antipodal to the mean of R-polarity dykes. Group I (GI) comprises nine N-polarity dykes with their mean at $D_m = 337.8°$, $I_m = -39.4°$ ($k = 130.7$, $\alpha_{95} = 4.5°$), and three dykes of R-polarity whose mean is at $D_m = 150.7°$, $I_m = 44.1°$ ($k = 147.1$, $\alpha_{95} = 10.2°$). The corresponding pole positions are at 43.5°S, 102.6°E ($A_{95} = 4.6°$) and 36.6°S, 107.6°E ($A_{95} = 8.9°$) respectively. These pole positions fall close to 65 Ma old Deccan Superpole (DSP) on the APWP, and may therefore be associated with magnetic Chron 29N for the N-polarity and 29R for the R-polarity of the three-Chron (30N–29R–29N) magnetostratigraphy of the Deccan Volcanic Province (DVP) used in the computation of DSP. In Group II (GII), eleven dykes display N-polarity with mean at $D_m = 312.6°$, $I_m = -45.2°$ ($k = 93.3$, $\alpha_{95} = 4.8°$) and six dykes show R-polarity with mean at $D_m = 130.1°$, $I_m = 48.0°$ ($k = 176.8$, $\alpha_{95} = 5.1°$). The corresponding pole positions at 25°S, 120.1°E ($A_{95} = 5.3°$) and 22.2°S, 119.1°E ($A_{95} = 5.2°$) respectively are significantly displaced (by more than 20°) from the DSP along the older segment (~80–90 Ma) of the Indian APWP. Hence, the dykes of GII appear to have been emplaced in an earlier episodic Deccan activity than that represented by the DSP. The palaeolatitudes corresponding to GI and GII are 23.2°S ± 4.0 and 27.6°S ± 4.5 respectively, indicating a latitudinal drift of ~4.4° of the sampled location between the acquisition of two magnetizations. Six lava flows sampled from the basement of the host Deccan flow sequence nearby sampled dykes yielded reverse polarity ChRM mean at $D_m = 128°$, $I_m = 47°$ ($k = 156$, $\alpha_{95} = 5.4°$) with corresponding pole positions at 21°S, 121°E ($A_{95} = 5.3°$). This pole falls near the GII poles, indicating a probable contemporaneous time of emplacement. In the absence of radiometric dates, no magnetochron can be assigned for GII magnetization. However, on the basis of published analyses of several palaeomagnetic and geochronological data of the flows and dykes within DVP and Deccan related dykes from the neighbouring areas, it seems plausible that GII–R magnetization belongs to either Chron 30R or 31R and GII–N magnetization pertains to 31N. Conclusive evidence in support of the presence of these reversals in the DVP, however, has to wait for new geochronological data from the undated dykes investigated in this study, and fresh updating of the stratigraphy of the lowermost flow sequence in the sampled area which also remains undated. This study, however, does indicate the possible presence of two more reversals revealed by GII magnetization on the older side beyond well-established three-Chron magnetostratigraphy.

Key words: Magnetostratigraphy; Palaeomagnetic secular variation; Palaeomagnetism; Reversals; Rock and mineral magnetism; Eruption mechanisms and flow emplacement.

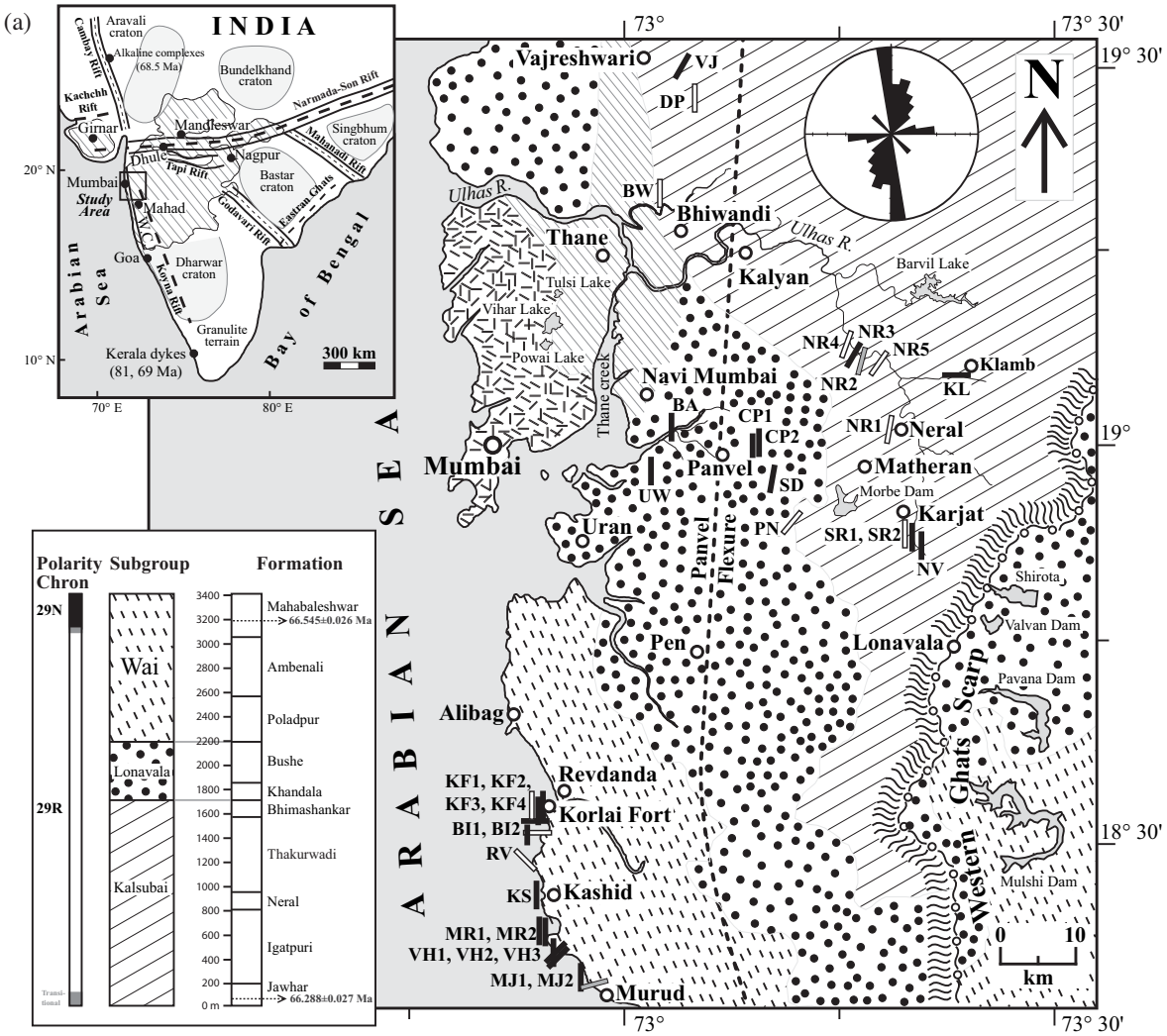

Figure 1. (a) Map of a part of the West Coast of India showing the axis of Panvel flexure and normal (solid bar) and reverse polarity (open bar) dyke sampling locations intruded into Kalsubai, Lonavala and Wai subgroups of the Deccan basalt group at north and south of Mumbai (modified from Subba Rao & Hooper 1988). Insets show: (top right) a Rose diagram of strike of sampled dykes; (top left) simplified map of peninsular India showing the major cratons and rift zones (Sheth 2005) and (bottom left) geomagnetic polarity timescale and composite stratigraphy column of the Deccan basalt subgroups and formations with U–Pb ages in the Western Ghats (modified from Schoene *et al.* 2015). (b) Typical field photographs of West Coast dykes (i–iv) that show tilting of the dykes SD, MJ1, NR3 and BI2 as details are given in Tables 1 and 3. (c) Field photographs of West Coast dykes: (i and ii) cross cutting N–S trending dykes by E–W dykes at Borlai (BI)–Korlai Fort (KF), ~50 km south of Mumbai, and (iii) two discriminating co-existed N–S trending dykes (SR1, SR2) at Karjat–Sireva village, ~50 km east of Mumbai. Refer panel (a) for locations and hammer for scale.

1 INTRODUCTION

The Deccan Volcanic Province (DVP), one of the world's largest provinces of continental flood basalts, covers the parts of central and western India between Latitudes 16°–24°N and Longitudes 70°–77°E. It extends into the Arabian Sea to the west sprawling over an area of 1.5 × 106 km^2 with an estimated original erupted volume of 1.3 × 106 km^3 (Jay & Widdowson 2008) and a suggested eruptive centre located to the north-east of Mumbai, where accumulation of flood basalt is up to 3000 m (Hooper 1990). As regards the origin of the Deccan flood basalts (e.g. Mahoney *et al.* 2002; Sheth 2005; Vanderkluysen *et al.* 2011), three different models have been proposed that include (1) the arrival of a mantle plume-head during the northward drift of the Indian plate followed by crustal extension (Richards *et al.* 1989; Campbell & Griffiths 1990; Campbell 1998; Courtillot *et al.* 2003; Ernst & Buchan 2003; Campbell 2005), (2) continental extension that preceded eruptions from the plume (White & McKenzie 1995) and (3) the model that does not require a mantle plume, and instead attribute vast basaltic extrusions to smaller-scale upper mantle convection related to craton boundaries and rift margins resulting in continental breakup and decompression melting (Sheth 1999a,b, 2005). Thus, the relative timing of rifting, separation of continental fragments, and Deccan volcanism is crucial to help evaluate models for the DVP.

From various geological and geophysical investigations, it has been suggested that the N–S Cambay rift and ENE–WSW Narmada–Son rift zones converging in western India (Biswas 1987) are the two major source regions from which Deccan lavas have poured out through tensional fractures (West 1959, 1981; Vanderkluysen *et al.* 2011; Fig. 1a). The Panvel flexure (Fig. 1a) is formed as a consequence of E–W extension that culminated in the post-Deccan rifting and separation of the Seychelles micro-continent (e.g. Hooper *et al.* 2010). The mafic dyke swarm comprising largely tholeiites and lamprophyres (Dessai *et al.* 1990;

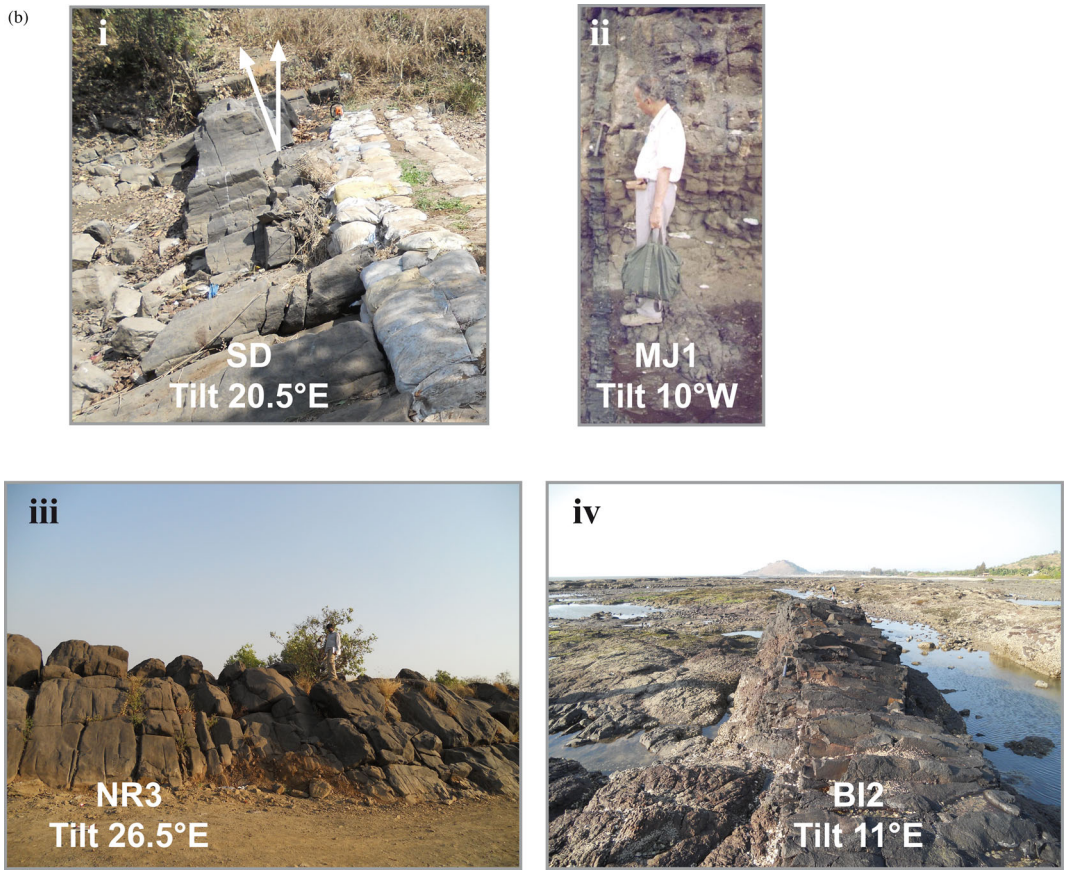

Figure 1. *(Continued.)*

Vanderkluysen *et al.* 2011) is intruded along the axial region of the Panvel flexure—the lamprophyres marked the cessation of magmatic activity. On the West Coast zone, the dykes are strongly N–S orientated and their emplacement can be linked to the rifting that resulted in the separation of the Seychelles from western India (Jerram & Widdowson 2005). Based on isotopic and geochemical characteristics, Vanderkluysen *et al.* (2011) and Hooper *et al.* (2010) inferred that the N–S dykes in the coastal area were a product of post-Deccan Seychelles rifting following the main phase of volcanism, and that the dykes with no preferred orientation in the Nasik-Pune swarm and coastal area were most likely feeders for the three main upper Formations (Fms) of the Wai subgroup (Poladpur, Ambenali and Mahabaleshwar). Moreover, Vanderkluysen *et al.* (2011) identified the dyke swarm as likely feeders for the lower and middle Fms (Fig. 1a) exhibiting preferred orientations consistent with the rifting based model, whereas the dyke swarms with no preferred orientation inferred to be the feeder dykes of the top Fms are inconsistent with the rifting model.

In view of the above reports on the dykes, it seems quite appropriate that tracing the magnetization history of the dyke swarms associated with different lava formations may enable us to understand further their links to rifting events and their timing of emplacement by observing changes in their magnetic signatures and polarities during volcanism. But, the palaeomagnetic investigations on the dyke swarms have so far been scanty, particularly dyke swarms along the West Coast within the DVP have not yet been adequately investigated to arrive at convincing inferences on the yet unsolved and controversial issues. Hence, we have investigated a larger number of dykes than in all other earlier palaeomagnetic studies with the objective of narrowing down some of the controversies related with Deccan volcanism.

1.1 Palaeomagnetic implications on the age and duration of Deccan flow stratigraphy

Early investigators classified the magnetostratigraphy of the flow sequence into only two polarity zones—one normal zone underlain by a thick sequence of reverse polarity zone (Deutsch *et al.* 1959; Wensink & Klootwijk 1971). This classification was, however, questioned by several investigators (e.g. Pal *et al.* 1971; Wensink 1973), who favoured more than two polarity Chrons based on their palaeomagnetic investigation of a large number of samples from thick sections of the Deccan sequence. From his palaeomagnetic results, Wensink (1973) concluded that Deccan lavas extruded during four successive polarity Chrons—two normal and two reverse ones, but not in rapid succession. He also concluded that there was fairly rapid drift of several tens of cm yr^{-1} which, he argued, was consistent with the interpretation of the magnetic anomalies in the Indian Ocean, where a rapid N–S spreading took place from anomaly 30 through anomaly 21. However, Vandamme *et al.* (1991) pointed out that these early studies used elevation to tie sections together which were incorrect because of the lava flows are in fact dipping slightly ($<1^{\circ}$), resulting in elevation offset over long distances between units of the same age.

The advent of the chemostratigraphy (e.g. Beane *et al.* 1986) helped to compare palaeomagnetic studies of the Deccan lava flows, and was used to correct previous magnetostratigraphy of the trap sections in the Deccan area. From joint consideration of

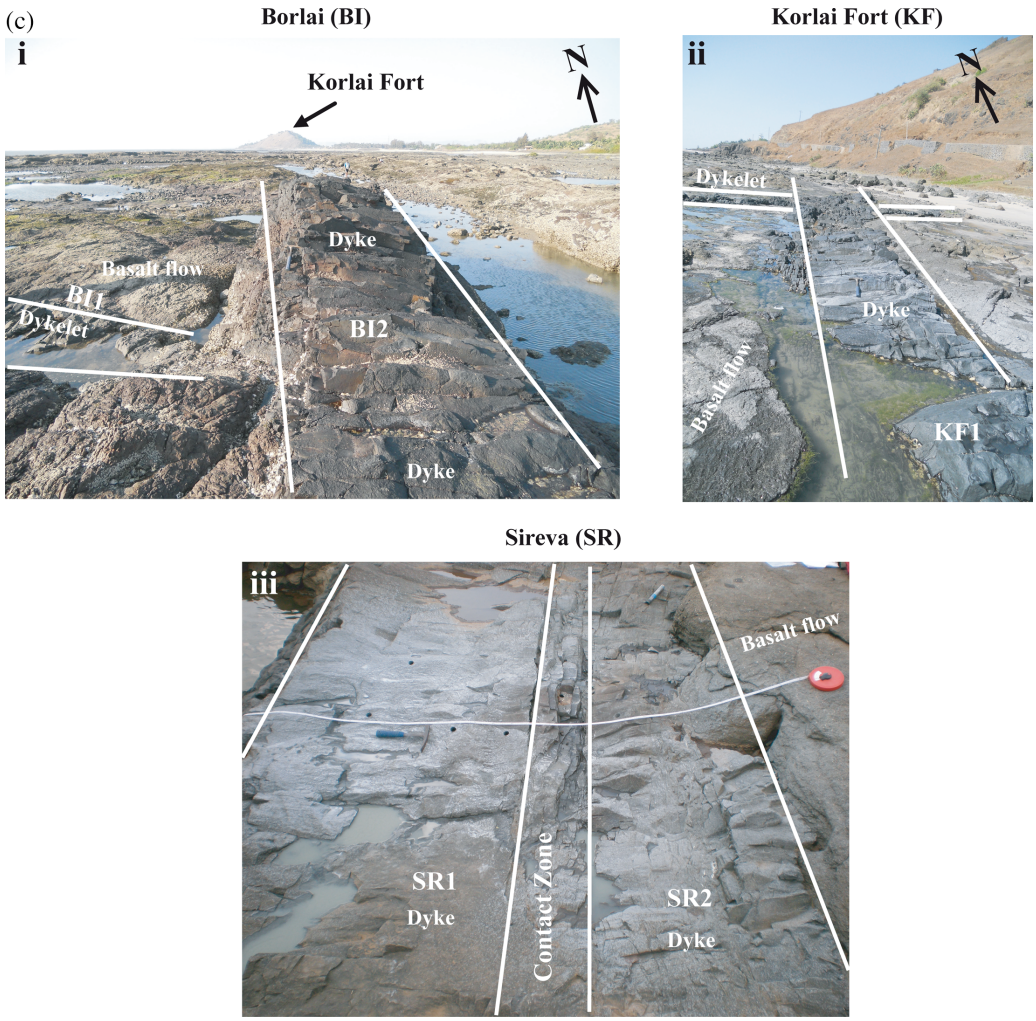

Figure 1. *(Continued.)*

geochronological, palaeontological and palaeomagnetic studies of the volcanic flows, which included review of all the available reliable data, Courtillot *et al.* (1986) conclusively inferred that Deccan volcanism of peninsular India (Fig. 1a) straddle only three magnetic Chrons—C30N, C29R, C29N with 80 per cent of the lavas having extruded during the reverse Chron 29R at Cretaceous/Palaeogene (K–Pg) boundary. They further concluded that the volcanic activity may have lasted <1 Ma. This conclusion of short duration and three-polarity Chrons centred at 29R was reinforced in the reports of Gallet *et al.* (1989), Vandamme *et al.* (1991) and Courtillot *et al.* (2000). Based on the compilation of all the reliable palaeomagnetic data, Vandamme *et al.* (1991) further proposed a Deccan Superpole (DSP) emphasizing the short duration of volcanism. This N–R–N magnetostratigraphy still remains the cornerstone of the timing and duration of Deccan volcanism.

However, several investigators have contradicted the above polarity sequence on the basis of their own studies and correlations of geochronological, geochemical and palaeomagnetic data on the flows, and have suggested a larger age bracket for the duration of volcanism that includes one or more reverse Chrons in the older side of the presently accepted N–R–N magnetostratigraphy of the flow sequence. In this context, Venkatesan & Pande (1996) considered the reliable ^{40}Ar–^{39}Ar ages of the basal part of the Western Ghats (WGs) and suggested that flows in this section may predate the K–Pg transition by ∼1.5 Ma, and that this section belongs to the 30R reverse polarity magnetic Chron rather than 29R as suggested by Courtillot *et al.* (1986, 1988). Notwithstanding the conclusions of Venkatesan & Pande (1996), the recent high-precision geochronology of the WGs showed that the basal part of the WGs is consistent in age with the ∼C30N/C29R transition, ∼400 ka before the K–Pg boundary (Renne *et al.* 2015; Schoene *et al.* 2015). Based on geochronological and palaeontological results (Chenet *et al.* 2007; Keller *et al.* 2008) combined with palaeomagnetic studies of the lavas, Chenet *et al.* (2009) have proposed that Deccan volcanism occurred in three short, discrete phases—an early one at ∼67.5 ± 1 Ma near the C30R–C30N reversal, which might have lasted only a few thousand years and after ca. 2.5 Ma of quiescence, the two larger occurred at ∼65 ± 1 Ma (one within C29R and the other at the boundary of C29R–C29N reversal). However, the new geochronological data of Renne *et al.* (2015) and Schoene *et al.* (2015) questioned the timing of eruption phases in the Deccan Traps evolution, and placed the bulk of eruption ∼66 Ma ago.

Thus from the above discussions, it may be concluded that there is a broad agreement in the investigations that Deccan volcanism was episodic in which bulk of lavas erupted in short pulses, close to or centred at ∼66 Ma over a period of ∼0.8–1.0 Ma. Recent Ar–Ar and U–Pb geochronology of the Deccan lava flows indicate that the main eruptive phase (>1.1 × 106 km^3 of basalts) initiated ∼250 ka

before and ended ∼500 ka after the K–Pg boundary (see Renne *et al.* 2015; Schoene *et al.* 2015). However, as a consequence of discovery of hiatus in extrusion episodes, and ongoing controversy in the age determinations and their correlations with the geochemical and palaeomagnetic data, the question of duration of Deccan volcanism in totality, and the number of geomagnetic field reversals preserved in the volcanic traps is still open.

It has been argued (Pande 2002; Pande *et al.* 2004) that a simplistic interpretation of magnetic stratigraphy data in terms of an N–R–N sequence everywhere in the Deccan is not supported by the available geochronological and palaeomagnetic database. However, the whole-rock Ar/Ar dates of Pande (2002) were low precision and occasionally produce spurious ages, >2 Ma, older than the eruption age (Baksi *et al.* 1996; Renne *et al.* 1998; Renne *et al.* 2015). For instance, the Bhimashankar Fm (premise for Pande *et al.* 2004) was redated in Renne *et al.* (2015) and has been shown to be consistent with eruption within C29R. Hence, the recent dating of the Deccan lava flows supports N-R-N magnetic stratigraphy in the Western Ghats. However, Chenet *et al.* (2007) pointed out a long hiatus in the eruptions to represent C30R/C30N or C31N/C30R based on integration of geochronological and magnetostratigraphy data. Although high precision geochronological data shows that all lava of reversed polarity in the WGs erupted within C29R (Renne *et al.* 2015 and Schoene *et al.* 2015), Chenet *et al.* (2007) showed the emplacement of Deccan flows spanned two reversal episodes corresponding to Chrons 30R and 29R, the former Chron was not recognized in the new geochronological data.

Even though the recent studies referred to above claim the presence of additional magnetic reversals in the Deccan flow sequence, there has been no unequivocal demonstration of this reversal by isolating stable magnetization either from the flow sequence or from the dykes anywhere in the DVP. In the present study, we are reporting stable normal and reverse magnetization from the West Coast dykes (WCDs) which is inferred to be related with an early phase of Deccan effusion implying a longer duration of volcanism than inferred in some of the studies mentioned above.

1.2 Status of palaeomagnetic studies on the Deccan dykes

Although palaeomagnetic studies on the flows in the DVP opened a new field in establishing their stratigraphic order of sequence based on N–R polarity (e.g. Deutsch *et al.* 1959; Wensink & Klootwijk 1971; Wensink 1987; Chenet *et al.* 2008; Jay *et al.* 2009), palaeomagnetic data on the Deccan dykes is very limited. Palaeomagnetic studies on the Deccan dykes so far reported include: (1) the Kutch dykes (Paul *et al.* 2008), (2) the Mandaleshwar dykes (Subbarao *et al.* 1988) and the E–W trending Dhule dykes (Prasad *et al.* 1996) in the Narmada–Tapti belt, (3) the NW–SE trending Murud dykes (Patil & Arora 2003) in the south of Mumbai, (4) the Goa NW–SE and NNE–SSW trending dykes (Patil & Rao 2002) on the West Coast of India and (5) the Deccan dyke swarms in southwest India (Radhakrishna *et al.* 1994; Radhakrishna & Joseph 2012). Whereas the palaeomagnetic data of Mandaleshwar dykes do not meet strict criteria of their acceptability, the rest of the above studies yield pole positions that are almost concordant with the DSP at 37°S, 101°E ($A_{95} = 2.4°$; Vandamme *et al.* 1991).

If we look at the dyke trends so far investigated in the above studies, we find that palaeomagnetic studies are mostly limited to the N–S and E–W trending dyke swarms. No information at all exists on the NE–SW and NW–SE dykes that outcrop near Mumbai. In the present study, therefore, dykes have been selected which trend in all possible directions within the DVP from Vajreshwari–Bhiwandi–Karjat–Mumbai–Alibag–Murud area (Figs 1a–c) to explore variations, if any, in the rock magnetic and palaeomagnetic signatures between their different trends of occurrence. Furthermore, since palaeomagnetic data has so far indicated unresolvable time difference between the emplacement of flows and intrusion of dykes into them, one of our objectives in enriching the dyke data has been to see if indeed there is any significant time difference between this post-flow event and the flow sequence. Besides, palaeomagnetic data from the dykes may provide additional information on the magnetostratigraphy of the Deccan sequence and duration of volcanism alongside the flow data.

Hence, with a view to get some insights into these aspects, we report here our investigation on the rock magnetism and palaeomagnetism of basement dykes and lava flows sampled along the West Coast around Mumbai. The dykes under investigation include one lamprophyre dyke from Murud (MJ1), which has the Rb–Sr date of 64.9 ± 0.8 Ma (Sahu *et al.* 2003) and for the remaining dykes we do not have radiometric dates. Knight *et al.* (2000) also reported biotite-whole rock Rb–Sr ages of ∼63–64 Ma for the lamprophyres of the Murud region. The temporal link of other studied dykes and Deccan Traps may be suggested from a comparison between available radiometric data of Deccan-age dykes from Kerala–Karnataka, main DVP and Kutch regions (e.g. Kaneoka 1980; Radhakrishna *et al.* 1994; Hofmann *et al.* 2000; Widdowson *et al.* 2000; Kumar *et al.* 2001; Sahu *et al.* 2003; Paul *et al.* 2008; Hooper *et al.* 2010; Radhakrishna & Joseph 2012) and published palaeomagnetic results (Wensink 1973; Klootwijk & Peirce 1979; Vandamme *et al.* 1991) with similar palaeomagnetic directions of the present study. We have discussed the implications of results from this study in the light of the present state of knowledge on the duration of volcanism and magnetostratigraphy of the Deccan flow sequence as reported in the previous studies of the dykes and lava flows.

2 GEOLOGY AND SAMPLING

2.1 Regional geology, locations, samples and methods

In the Indian geology, the youngest recognized stratigraphic event was the Deccan volcanic eruptions. Notwithstanding different viewpoints on the origin of eruptions, the main Deccan basalt group lavas in the WGs sections are divided into three subgroups and 12 Fms based on their stratigraphy, chemical and isotopic compositions (e.g. Devey & Lightfoot 1986; Subbarao & Hooper 1988; Mitchell & Widdowson 1991; Saunders *et al.* 2007). Palaeomagnetic studies on these Fms indicate a thick lava pile with the lower 3.5 km showing reverse polarity overlain by normal polarity flows, for example, Mahabaleshwar, Panhala and Desur Fms of the youngest Wai subgroup (e.g. Chenet *et al.* 2007; Jay & Widdowson 2008). Transitional and normal polarities are also seen in basal Fms (i.e. Jawhar) within the WGs (see Vandamme *et al.* 1991; Chenet *et al.* 2009). The present investigation of a Deccan dyke swarm is undertaken as a sequel to palaeomagnetic studies of the basalt flows.

Although the Deccan basalt occurs predominantly in the form of lava flows, many igneous intrusions such as plutons, regional dyke swarms, sills and late-stage trachytes do also occur in the western and central regions of the Deccan (Sen 1995). We emphasize that understanding of the relationship between Deccan dyke intrusions and flows remains at a very preliminary level (e.g. Beane *et al.* 1986; Hooper 1990; Bhattacharji *et al.* 1996). Many workers (e.g. Ray *et al.* 2007; Hooper *et al.* 2010; Vanderkluysen *et al.* 2011) have

explained that the erupted Deccan Traps (DTs) were mostly fed by the dyke intrusions. From the geochemical analysis, Vanderkluysen *et al.* (2011) and Hooper *et al.* (2010) concluded that three main episodes of dyke injections occurred, those that fed the main tholeiitic succession exposed in the WGs to the east, a later phase of basaltic injection associated with the onset of crustal extension and producing a return Thakurwadi-type chemical signature and a final phase of more alkaline and/or lamprophric dykes associated with the rifting of the Seychelles post main phase Deccan volcanism. Although geochemistry has been useful in defining stratigraphic units of basaltic lavas (e.g. Hooper *et al.* 2010), combined approaches yield great success (e.g. Chenet *et al*. 2008, 2009; Jay *et al.* 2009). Herein we examine the geochronological and palaeomagnetic data (magnetostratigraphic studies) related to the dykes that have been intruded in the large areas of DVP along the western margin of India.

The present study area of Mumbai is located west of the WGs escarpment (Fig. 1a), and exposes the basalt flows dipping west at 5–25° and are part of the Panvel flexure, which is a late-stage tectonic structure on the western Indian rifted margin (Melluso *et al.* 2002; Pande *et al.* 2017; Samant *et al.* 2017). The westerly dipping (17–18°) coastal lava flows in the Panvel flexure zone were intruded by numerous dykes with a strong preferred orientation (N–S, NNW–SSE and NNE–SSW; e.g. Auden 1949; Dessai & Viegas 1995; Sheth *et al.* 2014; Pande *et al.* 2017; Fig. 1a). These coastal dykes were earlier studied for their geology (e.g. Deshmukh & Sehgal 1988; Dessai & Viegas 1995; Melluso *et al.* 1999; Sethna 1999), geochemistry (e.g. Saunders *et al.* 2007; Hooper *et al.* 2010; Vanderkluysen *et al.* 2011) and geochronology (e.g. Hofmann *et al.* 2000; Knight *et al.* 2000; Sahu *et al.* 2003). In terms of intrusive age, the dykes belong to four groups in the WCD swarm (Dessai *et al.* 1990; Dessai & Bertrand 1995; Dessai & Viegas 1995). The dykes cropping out along the coast north and south of Mumbai are found that majority of dykes showed tilt angles ranging from 1 to 13°, while few dykes exhibit tilt ∼20° (Table 1, Fig. 1b). Along the entire length of the Panvel flexure zone, there are numerous N–S trending dykes, which were tilted tectonically after emplacement because the lava pile in this area dips to the west (e.g. Sheth 1998; Melluso *et al.* 2002; Pande *et al.* 2017; Samant *et al.* 2017).

Our study area of the WCD swarm is situated along the coast in the north and south of Mumbai and northeastern Konkan area (Fig. 1). Oriented samples for palaeomagnetic study were collected from 33 dykes cutting exposures along the coast, rocky beach stretches, quarry sites, road cuts and river banks. These dykes are best exposed at the base of WGs and occur in variable orientations of N–S, E–W, NE–NW and NW–SE between 18°18′43.6″ to 19°28′44.2″N and 72°57′31.9″ to 73°19′ 46.1″E (Fig. 1). It is also possible that small tilts may be useful in inferring the palaeomagnetic data as a pre-tilting or post-tilting magnetization. Locations, coordinates, field relations such as width, trend and tilt angles and petrographic observations of the dykes analysed are presented in Table 1. Fig. 1(a) shows the location of WCD swarm with a rose diagram showing preferred orientations of the dyke trends, the N–S axis of the Panvel flexure and the composite stratigraphy (after Schoene *et al.* 2015) of the western Deccan basalt Fms along which the dykes might have been emplaced.

Of the oriented samples collected from 33 dykes, 15 dykes intrude the younger Wai subgroup while 6 and 12 dykes intrude the older Lonavala and Kalsubai Fms respectively (Fig. 1). Almost all the dyke and flow samples were collected from fresh and unweathered exposures from the centre of dykes and were completely free of vesicles and secondary minerals. Two sets of dykes were sampled—the relatively larger ones (up to >1 m wide) of variable orientation and the smaller dykes (<1 m wide) of nearly N–S strike (Fig. 1 and Table 1). The access along the coast was largely limited by the time of low tides in order to sample the basement lavas and dyke intrusive rocks. In the sampled dykes, a lamprophyre dyke from Murud (MJ1) intruded into the basalt flows exposed on the wave-cut section and has ^{87}Rb–^{86}Sr date of 64.9 ± 0.8 Ma (Sahu *et al.* 2003), and ^{40}Ar–^{39}Ar date of 65.2 ± 0.4 Ma for a basalt dyke (not sampled here) cutting across the Poladpur Fm of the WCD swarm underlying topmost Mahabaleshwar Fm (Hofmann *et al.* 2000). As these dykes are intruded into the R-polarity Poladpur Fm of Wai subgroup (Fig. 1), they should be younger than the Poladpur Fm and should be hypabyssal intrusive (Powar & Vadetwar 1995).

The order of cross-cutting relations establishes a relative chronology between the dyke trends. The E–W trending mafic dyke (BI1) of Borlai village exhibits a cross-cut pattern by N–S dyke (BI2; Figs 1c-i), suggesting that the Deccan volcanism is episodic in nature. Careful field observation suggests that the N–S dykes could be younger in age because they intersect the E–W dyke. However, N–S dyke KF1 is older cross-cutting younger E–W dyke (Fig. 1c-ii). There are also examples of the N–S dykes being either intersected by SE–NW or E–W dykes or by SE–NW fractures.

Additionally, the NE–SW dykes in the Vihoor–More areas have SE–NW cross-cutting fractures. The strict parallelism of Deccan dykes with the observed fracture systems suggests that these fractures could be the channel ways for the emplacement of these dykes. The observed cross-cutting relationships between the dykes and fracture systems in this study thus indicate that the N–S and E–W trending fracturing and dyke activities could be contemporaneous. The two co-existed N–S trending dykes (SR1–2) at Sireva across Ulhas River run parallel to each other indicating the significance of weak contact zones in the pulsatory nature of Deccan volcanism during the emplacement of dykes (Fig. 1c-iii).

Detailed field characteristics with co-existent and cross-cutting pattern of the WCD swarm recognize the evidence for two distinct dyke events (Fig. 1c). In view of this, the intrusive age of the sampled dykes can then be attributed to the occurrence of several eruptive cycles with the time span covered by each magmatic dyke cycle being variable. The palaeomagnetic analyses might be expected to give more information about the temporal effects on the formation of different dyke swarms. This is based on magnetic polarity that relates the coastal swarm dykes with a particular emplacement period, an event likely to be associated with opening and closing phases of eruption of Deccan flood basalts. As the ages of the studied WCD swarm are poorly constrained, palaeomagnetic and magnetostratigraphic constraints may sort out their distinctive emplacement history during Deccan volcanism.

2.2 Palaeomagnetic sampling and sample preparation

Altogether 194 palaeomagnetic cores from 33 dykes (sites) were drilled by a portable gasoline-powered drill fitted with a water-cooled diamond bit (Stihl, USA) and a coring tube of 2.5 cm inner diameter. After being drilled, each core was oriented by placing an orienting device consisting of a Brunton compass and a levelling table into the drill hole and measuring its plunge and plunge of the drill direction with a magnetic compass and inclinometer. The accuracy of orientation, for example, dip and azimuth is about ±2°. Effects of strongly magnetized volcanic rocks of the DTs were minimized by measuring azimuth at ∼0.3 m distance over the dyke. After preliminary palaeomagnetic measurements of representative

Table 1. GPS locations of palaeomagnetic data sampling sites of West Coast dyke swarm near Mumbai with site specifics of strike, tilt, thickness, local geology and microscopic observations.

Sub group	Formation	Sample	Locality	Location		Strike	Tilt (°)	Tilt towards	Dyke width (m)	Geology and microscopic observations
				Lat. (N)	Long. (E)					
Wai	Poladpur	MJ1	Murud-Janjira	18°18′43.6″	72°57′31.9″	N–S	10.0	West	0.2	Two sets of dykes of fine-grained basaltic composition containing phenocrysts of subhedral prismatic plagioclase and rare olivine. Lamprophyre dyke dated to 64.9 ± 0.58 Ma (Sahu *et al.* 2003) and 66–63 Ma (Knight *et al.* 2000) by Rb-Sr method.
		MJ2		18°18′56.0″	72°57′21.7″	N75E	–	–	4.5	
		MR1	More	18°20′58.4″	72°55′41.1″	N20E	No tilt	East	0.6	N–S and NNE–SSW trending two olivine porphyritic basalt dykes.
		MR2		18°20′01.0″	72°55′45.4″	N9E	10.0	West	1.0	
		VH1	Vihoor	18°21′01.5″	72°55′47.5″	N10E	5.0	East	0.6	NNE–SSW and NE–SWE olivine porphyritic basaltic dykes showing cross-cutting fractures that could be channel ways for their emplacement.
		VH2		18°21′01.0″	72°55′50.0″	N50E	10.6	East	0.6	
		VH3		18°21′01.0″	72°55′50.3″	N22E	1.5	East	0.7	
		KS	Kashid	18°25′27.0″	72°54′30.1″	N16E	2.0	East	0.7	Basic dykes of olivine porphyritic basalt showing a length parallel fracture along with two sets of transverse fractures trending ENE–WSW and ESE–WNW. This dyke dated to 65.3 ± 0.4 by Amphibole-whole rock $^{40}Ar/^{39}Ar$ method-Hofmann *et al.* (2000).
		RV	Revadanda	18°29′44.5″	72°54′15.4″	N315W	No tilt		3.6	SE–NW trending fine-grained basalt dyke showing features of basaltic melt locally.
		BI1	Borlai	18°30′46.3″	72°54′35.8″	E–W	3.0	East	1.1	E–W mafic dykes cross-cut by N–S dykes containing plagioclase and pyroxene phyric basalt.
		BI2		18°30′46.2″	72°54′35.4″	N–S	11.0	East	2.0	
		KF1	Korlai Fort	18°32′20.5″	72°54′17.6″	N–S	13.0	West	3.9	N–S dyke overlain by younger Deccan flows indicating they could predate the overlying lava flows. The dykes in this area are either dolerite or olivine phyric basalt, or olivine of plagioclase phyric of extremely fine-grained basalt.
		KF2		18°31′51.2″	72°55′12.8″	N15E	4.7	East	2.2	
		KF3		18°32′14.9″	72°56′17.9″	N–S	7.0	West	1.5	
		KF4		18°32′17.2″	72°54′17.8″	E–W	8.0	East	1.9	
Lonavala	Khandala	PN	Panshil	18°54′27.0″	73°12′36.1″	N20E	12.0	East	3.0	
		SD	Shedung	18°57′40.8″	73°10′21.4″	N9E	20.5	East	6.0	
		UW	Ulwe	18°58′08.5″	73°01′28.8″	N11E	20.0	East	5.4	
		CP1	Panvel-Matheran	19°00′15.8″	73°08′51.4″	N10E	17.0	East	1.9	Dyke samples have fresh olivine and rare plagioclase crystals embedded in the glassy groundmass, which is dark due to enrichment in opaque minerals and secondary alterations.
		CP2		19°00′15.8″	73°08′51.4″	N7E	14.0	East	10.5	
		BA	Belapur	19°01′19.9″	72°02′54.2″	N5E	19.7	East	5.0	

Table 1. *(Continued.)*

Sub group	Formation	Sample	Locality	Location		Strike	Tilt (°)	Tilt towards	Dyke width (m)	Geology and microscopic observations
				Lat. (N)	Long. (E)					
Kalsubai	Thakurwadi	BW	Biwandi	19°18′54.7″	73°01′45.4″	N–S	10.0	West	1.0	
		DP	Dugurpada	19°26′25.5″	73°04′10.5″	N–S	No tilt		6.5	
		VJ	Vajreswari	19°28′44.2″	73°03′44.2″	N30E	No tilt		2.5	
Kalsubai	Neral	NV	Nevali	18°52′58.7″	73°20′08.4″	N5E	30.0	East	4.3	Basalt dykes with ground mass of plagioclase laths and interstitial pyroxene and glass.
		SR1	Sireva	18°53′19.9″	73°19′46.1″	N13E	8.5	West	1.6	
		SR2		18°53′19.9″	73°19′46.1″	N–S	12.0	West	1.3	
		NR1	Neral	19°01′51.0″	73°18′46.0″	N14E	12.0	East	18.9	
		NR2		19°06′48.7″	73°16′32.4″	N22E	3.0	West	20.0	
		NR3		19°06′52.8″	73°16′26.0″	N33E	26.5	East	33.0	
		NR4		19°07′54.0″	73°15′48.3″	N20E	8.5	West	5.5	
		NR5		19°06′42.5″	73°16′49.5″	N30E	13.5	West	15.0	
		KL	Kalamb	19°05′32.8″	73°23′15.2″	N88E	13.5	East	9.0	E–W fine-grained basaltic dyke containing cm-sized xenoliths, subhedral phenocrysts, prismatic plagioclase and magnetite.

samples leading to the identification of normally and reversely magnetized dykes, sampling sites were revisited to collect samples from host lava flows adjacent to a few reversely magnetized dykes to establish their reverse polarity in the lower part of the lava succession through which they cut, given the main succession inland of Mumbai has been established as reversed (Chron 29R) by previous workers (e.g. Renne *et al.* 2015; Schoene *et al.* 2015). Hence, this study may help to establish relationship between the flows and dykes in respect of their characteristic directions and magnetic polarities in the established Deccan stratigraphy. At majority of sampling sites, in situ tilt angles of dykes with respect to nearby west-dipping flows were measured and recorded. Tilt corrections were used to establish whether remanences were pre- or post-tilting due to a regional Panvel flexure (Fig. 1).

In the laboratory, five to eight cores from 33 dykes and six lava flows were sliced into standard 2.5 cm diameter and 2.2 cm length specimens using a water-cooled dual diamond-blade saw (ASC Scientific, USA), yielding a total of 388 dyke and 68 basal flow specimens. Once the specimens were prepared, their characteristic magnetizations were isolated from >5 to 26 specimens from each dyke and flow sites, which were then analysed using Fisher's (1953) statistics. All the palaeomagnetic and rock magnetic measurements were carried out at the Indian Institute of Geomagnetism, Navi Mumbai, India.

3 LABORATORY MEASUREMENTS

The natural remanent magnetization (NRM) was measured using an AGICO JR-6A dual-speed spinner magnetometer having a high speed sensitivity of 2×10^{-6} A m^{-1}. The samples were subjected to alternating field (AF) demagnetization in 15 incremental steps (2.5–100 mT) by using ASC Scientific D–Tech AF demagnetizer and thermal demagnetization using MMTD80 in 11 steps up to 600 °C. All measurements were processed using the PMAGIC software (Rehacek 1994) to obtain the palaeomagnetic information.

To characterize magnetic mineral phases and the size of magnetic mineral grains in WCD samples, various rock magnetic measurements and their ratios were carried out: (i) magnetic susceptibility (χ) using AGICO MFK1-FA Kappabridge, (ii) anhysteretic remanent magnetization (ARM) by imparting a bias DC field of 0.05 mT superimposed on a peak AF of 100 mT with ASC's D–Tech AF demagnetizer, (iii) Stepwise acquisition of isothermal remanent magnetization (IRM) in a forward field up to 1 T and stepwise demagnetization in backfield up to 300 mT using a MMPM9 Pulse Magnetizer and a Spinner Molspin/JR-6A magnetometer, (iv) Variation of magnetic susceptibility with temperature (χ–T) at incremental temperatures during heating and cooling cycles (–196 to 700 °C) using AGICO KLY-4S Kappabridge connected to low (high) temperature CS-L (CS-3 in argon atmosphere) furnace, and (v) Hysteresis study using a MicroMag Alternating Gradient Magnetometer (AGM) in fields cycling between ±1 T, respectively.

4 RESULTS AND INTERPRETATION

4.1 Rock magnetic results

The bulk magnetic properties of all dyke and flow samples from the West Coast near Mumbai reveal consistent variations of magnetic concentration (χ, ARM, SIRM), grain-size (ARM/SIRM, SIRM/χ) and composition (Soft IRM, Hard IRM, S-ratio) and it is likely that uniform grain-sized ferrimagnetic mineral phase is the only

Table 2. Rock magnetic parameters related to the concentration, grain-size and composition for West Coast dyke swarm and basement lava flows.

Dyke/flow	Concentration			Grain-size		Composition		
	$\chi \times 10^{-7}$ ($m^3\ kg^{-1}$)	ARM $\times 10^{-5}$ ($A\ m^2\ kg^{-1}$)	SIRM $\times 10^{-3}$ ($A\ m^2\ kg^{-1}$)	ARM/SIRM $\times 10^{-3}$	SIRM/$\chi \times 10^3$ ($A\ m^{-1}$)	Soft IRM $\times 10^{-3}$ ($A\ m^2\ kg^{-1}$)	Hard IRM $\times 10^{-3}$ ($A\ m^2\ kg^{-1}$)	S-ratio
MR1	109.7	126.3	314.1	4.0	28.6	260.6	4.63	0.99
MR2	31.9	60.9	112.4	5.4	35.2	78.9	2.43	0.98
VH1	47.8	78.8	48.2	16.3	10.1	14.8	2.57	0.95
VH2	34.7	143.8	88.2	16.2	25.4	42.4	4.36	0.95
VH3	35.5	80.1	107.3	7.5	30.3	101.8	0.02	1.00
KF2	215.7	148.1	179.3	8.3	8.3	165.1	3.04	0.98
KF3	128.0	66.9	139.8	4.8	10.9	105.5	0.09	1.00
KF4	47.3	68.6	42.1	16.3	8.9	33.1	0.69	0.98
MJ1	240.0	121.3	149.5	8.1	6.2	30.9	0.72	1.00
BI2	137.9	109.8	41.8	26.3	3.0	2.4	0.26	0.92
KS	27.6	85.3	89.7	9.5	32.5	73.3	0.56	0.99
BA	116.3	121.6	53.7	22.7	4.6	10.7	0.31	1.00
UW	100.1	508.0	276.5	18.4	27.6	225.6	3.98	0.99
SD	25.2	85.4	37.4	22.8	14.8	16.3	0.48	0.99
KL	144.7	106.2	142.5	7.5	9.9	78.3	0.40	0.97
NV	65.7	61.7	176.9	3.5	26.9	104.4	5.07	0.97
SR2	175.3	189.4	151.9	12.5	8.7	28.3	2.74	0.98
NR3	54.3	76.2	145.5	5.2	26.8	107.0	1.17	0.99
VJ	141.7	139.1	133.4	10.4	9.4	14.6	1.69	0.99
PM1	72.2	77.7	51.1	15.2	7.1	12.4	0.54	0.99
PM2	66.3	49.3	55.1	8.9	8.3	13.7	1.59	0.97
BI1	193.6	120.6	129.3	9.3	6.7	57.1	0.13	1.00
KF1	167.8	104.5	133.2	7.9	7.9	58.9	1.31	0.99
RV	106.6	88.8	314.1	2.8	29.5	171.8	10.32	0.97
PN	146.1	254.3	140.4	18.1	9.6	26.6	3.43	0.98
SR1	69.5	114.8	241.6	4.8	34.8	194.2	1.58	0.99
NR1	217.8	224.0	73.9	30.3	3.4	11.0	1.03	0.99
NR4	158.5	230.5	66.5	34.7	4.2	4.3	0.74	0.98
NR5	44.9	304.3	124.5	24.4	27.7	57.6	2.08	0.98
DP	138.0	88.2	107.7	8.2	7.8	13.1	0.16	1.00
BW	261.4	705.1	395.3	17.8	15.1	385.9	0.13	1.00
NR2	168.7	124.7	120.7	10.3	7.2	17.5	0.95	0.99
MJ2	107.4	126.2	137.1	9.2	12.8	70.1	0.77	0.99
KF1F[a]	131.3	134.1	548.2	2.4	41.8	286.3	4.16	0.99
RVF[a]	95.9	91.6	169.5	5.4	17.7	158.0	4.09	0.98
PNF1[a]	88.8	67.0	128.8	5.2	14.5	81.6	8.88	0.93
PNF2[a]	57.6	40.3	113.5	3.5	19.7	76.3	6.15	0.95
DPF[a]	100.7	59.3	104.3	5.7	10.4	86.1	6.48	0.94
BWF[a]	61.4	71.8	573.2	1.3	93.4	116.0	47.94	0.92

χ, magnetic susceptibility; ARM, anhysteretic remanent magnetization; SIRM, saturation isothermal remanent magnetization; Soft IRM, SIRM–$IRM_{-0.03T}$; Hard IRM, SIRM–$IRM_{-0.3T}$; S-ratio, $IRM_{-0.3T}$/SIRM.
[a]Deccan flow.

magnetic carrier in these dykes. Results from analyses of the magnetic mineral components contained in the dyke samples are shown in Table 2. All samples saturate at 0.3 T showing a rapid rise by <200 mT (Fig. 2a), suggesting minor contributions of hematite and that the magnetic carriers are most likely fine-grained Ti-magnetite and magnetite. This result is in accordance with coercivity of remanence (B_{cr}) values ranging between 15 and <100 mT (inset Fig. 2a) and a dominant Soft IRM over Hard IRM (Table 2). The S-ratios, simplified here as $IRM_{-0.3T}$/SIRM, predominantly range from 0.97 to 1.0, indicating Ti-magnetite as the predominant remanence carrier in DT basalt sources, which are identified by a narrow range of high S-ratio values (Fig. 2b; Basavaiah & Khadkikar 2004; Basavaiah *et al*. 2010, 2015; Basavaiah 2011).

The presence of Ti-magnetite and its oxidation products is documented in the high-temperature χ–T curves, which are characterized by major drops in χ within <580 °C (Figs 2c–e). Furthermore, variation of χ between liquid nitrogen (−196 °C) and room temperature (27 °C) reveals signs of Ti-magnetite poor in Ti and Ti-magnetite rich in Ti and their grain-size distribution in the samples (Figs 2c–e). The Curie temperatures (T_C) of samples from different dykes exhibit three types of thermomagnetic behavior: (i) high temperature χ–T curves showing a single phase of Ti-poor Ti-magnetite, usually resulting in $T_C \sim 550$ °C (Fig. 2c); (ii) two χ-peaks showing two components of Ti-rich ($T_C \sim 350$ °C) and Ti-poor ($T_C \sim 580$ °C) phases with possible maghemite (Fig. 2d), and (iii) a rapid increase of χ from −196 °C to higher temperatures and abruptly falling down at 100 °C with $T_C \sim 200$–300 °C that reveal predominant Ti-rich Ti-magnetite and a minor Ti-poor Ti-magnetite (T_C ∼550–580 °C) phases (Fig. 2e). In all samples, the cooling curves have a marked lower χ than the heating curve, possibly indicating some low temperature oxidation (LTO) of the Ti-magnetite (Figs 2c–e). Hence, the differences in T_Cs may be related to varying LTO degree of the Ti-magnetite with variable Ti contents as described by Basavaiah *et al*. (2010, 2015).

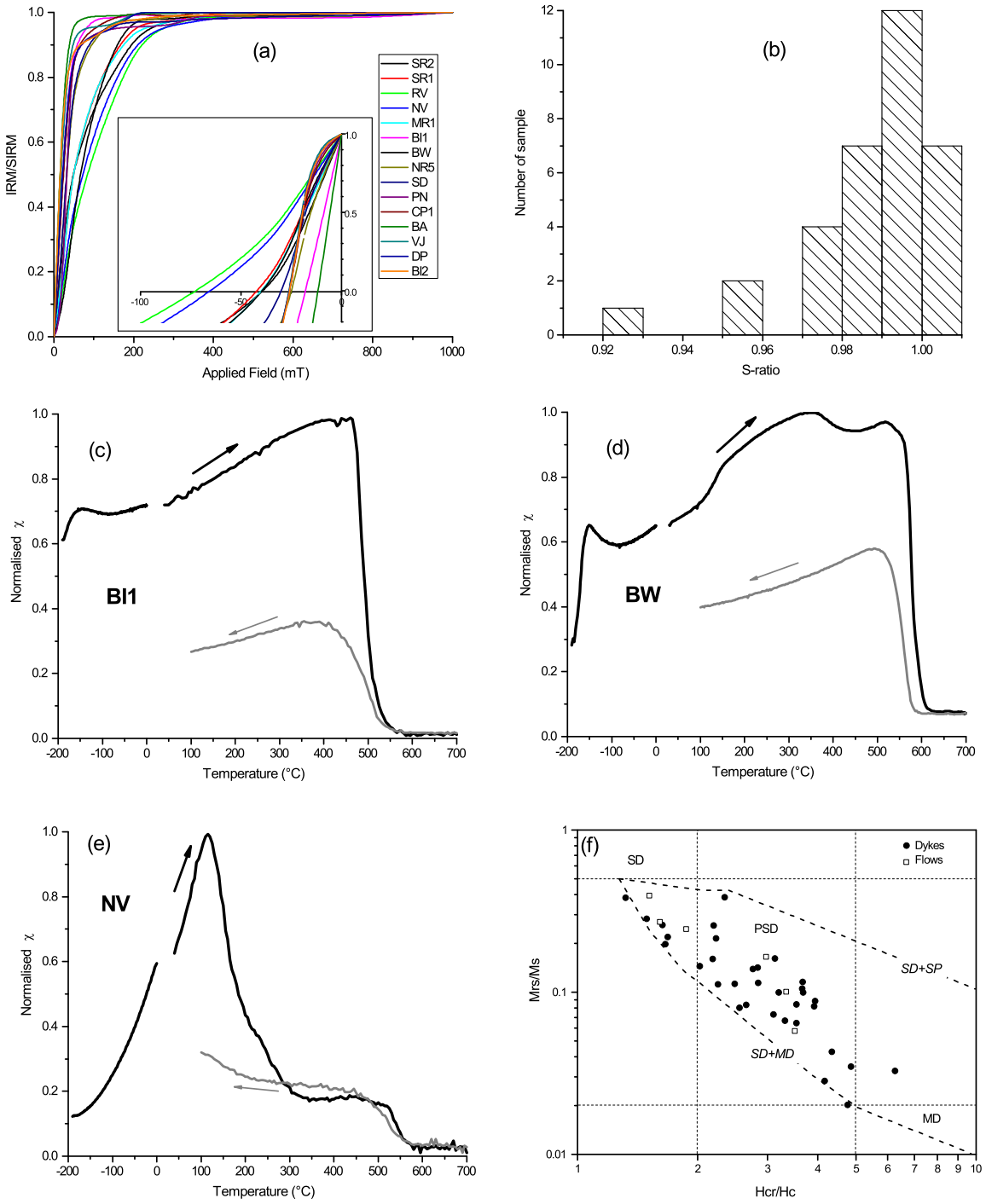

Figure 2. (a) Acquisition of isothermal remanent magnetization (IRM) together with coercivity (B_{cr}) of saturation IRM (SIRM) curves; (b) histogram of magnetomineralogical S–ratio ($IRM_{-0.3T}$/SIRM); (c–e) low and high temperature χ–T results with heating and cooling curves represented by arrows indicating the presence of titanomagnetites and their oxidation products and (f) Day plot of M_{rs}/M_s versus H_{cr}/H_c illustrating single–domain (SD) grains and majority in pseudo-single-domain (PSD) in West Coast dykes and flow samples.

The low-temperature χ behavior (Figs 2c–e) shows the Verwey transition (T_v) indicative of Ti-poor magnetite (Verwey 1939; Moskowitz *et al.* 1998; Chruch *et al.* 2011), and a steady increase in χ with temperature, suggesting the presence of magnetite in single-domain (SD; BI1 sample) and small pseudo-single-domain (PSD; BW sample) grains (Radhakrishnamurty 1993; Basavaiah 2011). The sample BI1 shows a broad reduced T_v which is consistent with SD magnetite grains, corresponding to partial oxidation of Ti-magnetite, while a sharp T_v peak (BW sample) points to multidomain (MD) or PSD magnetite grains with unoxidized compositions (Ozdemir *et al.* 1993; Radhakrishnamurty 1993; Moskowitz *et al.* 1998; Chruch *et al.* 2011). No other low temperature phase transitions are observed, and it is likely that Ti-magnetite is the only remanence carrier in these dykes (Figs 2c–e).

Being grain-size dependent, magnetic hysteresis loop parameters, for example, saturation magnetization (M_s), saturation

remanence (M_{rs}), coercivity (H_c) and coercivity remanenc (H_{cr}) provide a means of estimating magnetite grain-size in the dyke samples. An earlier study of hysteresis (Radhakrishnamurty 1993) on dykes SR1 and SR2 (investigated in the present study) exhibited wider Rayleigh loops in samples collected from the centre of the dykes than those collected from the edges or near the chilled margin. This indicates the presence of high coercivity grains characteristic of SD grain-size in the central region of the dykes. This observation prompted us to collect samples mostly from the centre of dykes for palaeomagnetic study. In the present study, however, hysteresis ratios M_{rs}/M_s plotted versus H_{cr}/H_c (after Day *et al*. 1977) range between 0.06–0.2 and 1.12–5.5 respectively (Fig. 2f). These ratios plot along a mixing trend of SD to PSD region close to the SD–MD mixture models (Dunlop 2002) of a Day plot. Hysteresis data suggest that the magnetic carriers within the dykes and flows are mainly SD or PSD. In conclusion, the rock magnetic results show an overall uniformity in magnetic mineral composition, suggesting the common association of titanium with the SD to PSD Ti-magnetite and magnetite in WCD swarm and basalts.

4.2 Palaeomagnetic results

4.2.1 Demagnetization and NRM stability tests

The intensity of NRM shows a broad range of variation from 1 to 18 A m^{-1} for dykes and from 1 to 6 A m^{-1} for flows. Two to three pilot samples per site (both dykes and flows) were subjected to AF and thermal demagnetization. In our study, AF demagnetization is found to be more effective than the thermal demagnetization in isolating the characteristic magnetic components. The AF treatment of 165 pilot specimens up to AF fields of 100 mT uncovered the most stable and consistent component of the characteristic remanent magnetization (ChRM) after removal of a viscous component in the lower AF fields up to 10 mT and some samples at >20 mT. Therefore, the rest of 326 specimens were subjected to reduced steps of demagnetization in AF fields between 10–60 mT. Samples from two dykes (MJ2, NR2) did not either show stable directions (MJ2) or gave quite a deviant ChRM (NR2) from the rest of the dykes, and hence, these dykes were dropped from further consideration. The ChRM directions are determined with principal component analysis (Kirschvink 1980) using orthogonal vector projections (Zijderveld plots) based on linear segments trending towards origin defined by at least four consecutive demagnetization steps at fields >30 mT with maximum angular deviation values <5°. Figs 3(a) and (b) show representative progressive demagnetized results on Zijderveld plots for typical dyke specimens that cut basal flows of the different lithological formations of the Deccan Traps stratigraphy (see Fig. 1a) with primary ChRMs.

On AF demagnetization, the specimens (BI, BA, SR, NV and VJ sites) reach a stable end point beyond 10 mT step and some above 20 mT step, while the specimens (RV, MR, PN, CP, BW and DP sites) show the uncovering of stable magnetization at >30 mT. Below 10 or 20 mT, the specimens exhibit superimposed viscous and soft components over the stable components. At higher demagnetization levels, a well-defined characteristic component trending SE and dips downwards for BI and RV dykes that were intruded into the Poladpur Fm, PN dyke in Khandala Fm, BW and DP dykes in Thakurwadi and NR dyke in Neral Fm (Fig. 3). However, BI2, CP1, VJ3 and NV3 dykes show characteristic component trending NW and dips upward in the respective Fms (Fig. 3). For specimens of RV, BW and NR dykes, the principal direction of magnetization trends towards origin, but does not reach the origin suggesting the specimens (RV and BW) contain high coercivity components (see Fig. 2 and Table 2). The magnetic polarities of ChRMs of different dykes do not agree with the established polarity of adjoining basement flows (see Fig. 1a).

4.2.2 Means of ChRM directions, tilting, pole positions and reversal test

Table 3 summarizes palaeomagnetic results for each dyke in this study together with their virtual geomagnetic poles (VGPs). The ChRM directions were isolated from 32 dykes out of 33 dykes with 21 dykes exhibiting N-polarity and 11 dykes showing R-polarity magnetization. Means of two R-polarity dykes (NR2 and NR5) and one normal polarity dyke (KF3) are widely scattered from the rest of the dykes of their respective polarity, hence they have not been included in the computation. Specimens from only six out of 12 basement flows close to R-dykes yielded stable directions, which exhibit reverse magnetization.

The correction for tilt of the studied dykes uses the dyke-attitudes such as strike, tilt angle and directions (see Table 1) following the mathematical algorithm of standard equations proposed by Enkin (2003). Since the dykes may have been tilted tectonically by Panvel flexural lineament (Figs 1a and b), a tilt correction is required to determine the ChRM direction with respect to horizontal. Hence, the tilt correction is performed by rotating the ChRM direction about the local dyke strike axis by the amount of the tilt of the dykes as given in Table 1.

Equal-area plots of dyke-means before and after tilt correction of the dykes are shown in Figs 4(a) and (b). The R-dykes yield a mean direction of $D_m = 136.1°$, $I_m = 46.4°$ ($k = 39.4$, $\alpha_{95} = 8.3°$, $N = 9$ sites) before, and $D_m = 137.2°$, $I_m = 47.1°$ ($k = 74$, $\alpha_{95} = 6.0°$, $N = 9$) after correction for the tilt. The mean direction for the N-polarity dykes is $D_m = 330.8°$, $I_m = -50.4°$ ($k = 29.9$, $\alpha_{95} = 6.1°$, $N = 20$ dykes) before correction for the tilt, and $D_m = 326.3°$, $I_m = -43.5°$ ($k = 36$, $\alpha_{95} = 5.4°$, $N = 20$) after tilt-correction. The mean direction from six flow sites close to R-polarity dykes are $D_m = 128°$, $I_m = 47°$ ($k = 156$, $\alpha_{95} = 5.4°$, $N = 6$ flows; Fig. 4f). Thus, dyke means for both the normal and reverse magnetization show well grouping (Figs 4a and b) after applying tilt-correction which is reflected by improvement in the statistical parameters after correction for the tilt (e.g. McElhinny 1964; McFadden & Jones 1981). This suggests the acquisition of magnetization to be pre-tilting of the dyke sequence which intruded into the west-dipping lava flows, and hence the tilt-corrected magnetization is probably primary.

The distribution of tilt corrected dyke-means on equal area plot (Figs 4b–d), however, do not appear to be Gaussian, rather it appears to be bimodal. This bimodal nature is more explicit in the normal ChRMs than in the Reverse ChRMs as seen in Fig. 4(b), probably because of fewer numbers in the latter. Since there is no evidence of the presence of any unremoved secondary NRM component in the individual specimen data following AF/Thermal cleaning, it appears that there was a significant movement of the geomagnetic field during the intrusion of dykes (Fig. 4e). With a view to a possible resolution of the temporal drift of the geomagnetic field from the bimodal non-Gaussian distribution of the VGPs, we decided to plot them on the Indian apparent polar wander path (APWP) which we discuss below.

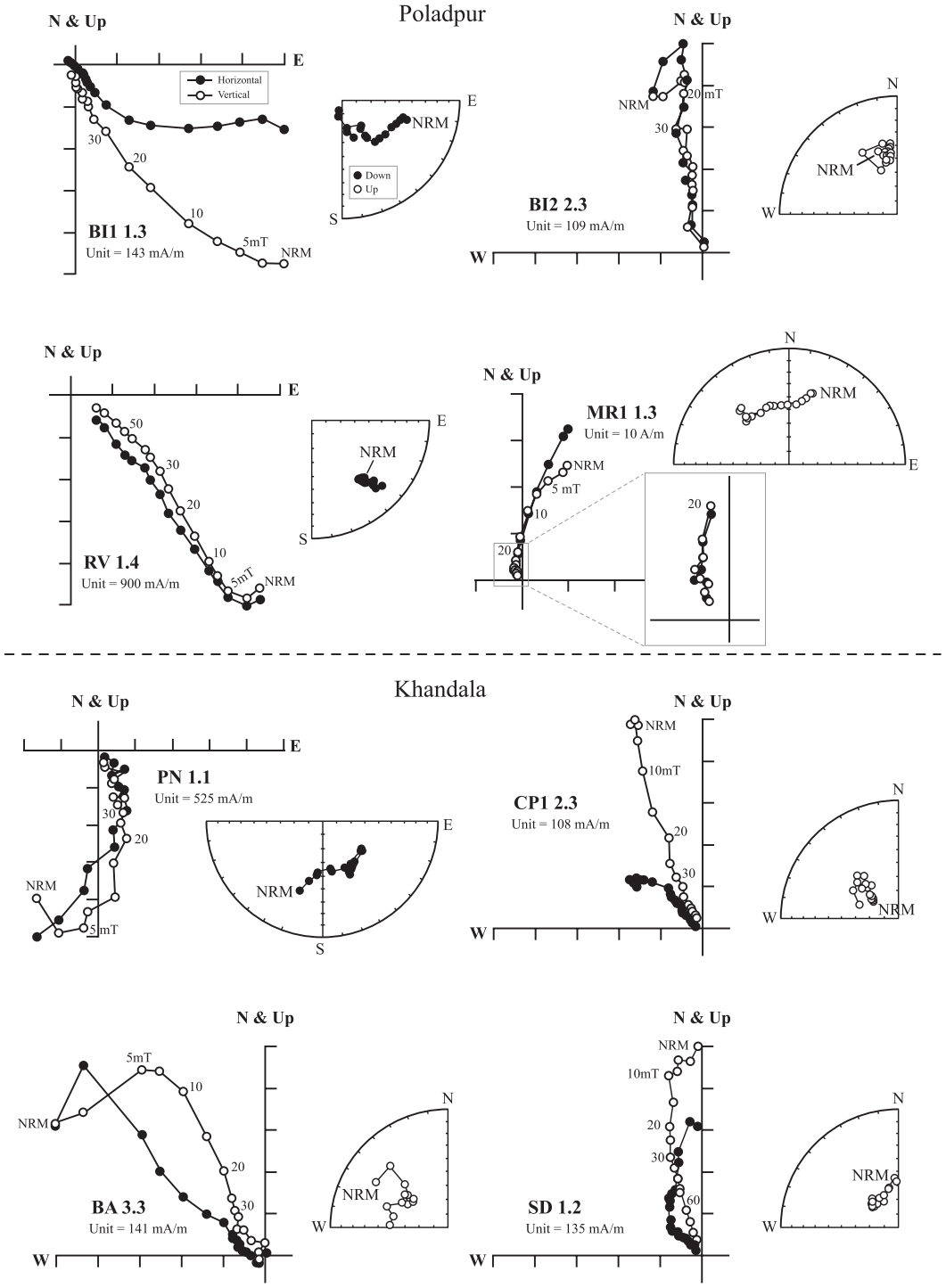

Figure 3. (a and b) The orthogonal vector (Zijderveld) diagrams and equal area projections showing representative results from Poladpur, Khandala, Thakurwadi and Neral formations during AF demagnetization. For vector diagrams, solid (open) circles are the horizontal (vertical) projections of remanent magnetization vector and for equal area projections solid (open) circles are projections on lower (upper) hemisphere at various steps of demagnetization. For AF demagnetization, the labelled steps are in millitesla (mT).

4.2.3 Grouping of VGPs over the Indian APWP

All the 29 VGPs were plotted on the Indian APWP (Klootwijk & Peirce 1979) with N-polarity and R-polarity VGPs plotted separately (Figs 5a and b), together with the well-established DSP. As seen in the plots, the VGPs form an oval distribution from the younger to older section of the APWP. Two clusters of VGPs are clearly seen on these plots. We have, therefore, attempted to classify the VGPs into two major well-defined groups, Group I (GI) and Group II (GII), according to their occurrence on the APWP. To form the two groups, we have chosen DSP as our reference point (Figs 5a and b), and all the VGPs which are within 20° of the DSP have been listed in GI and the rest are listed in GII. This criterion has yielded

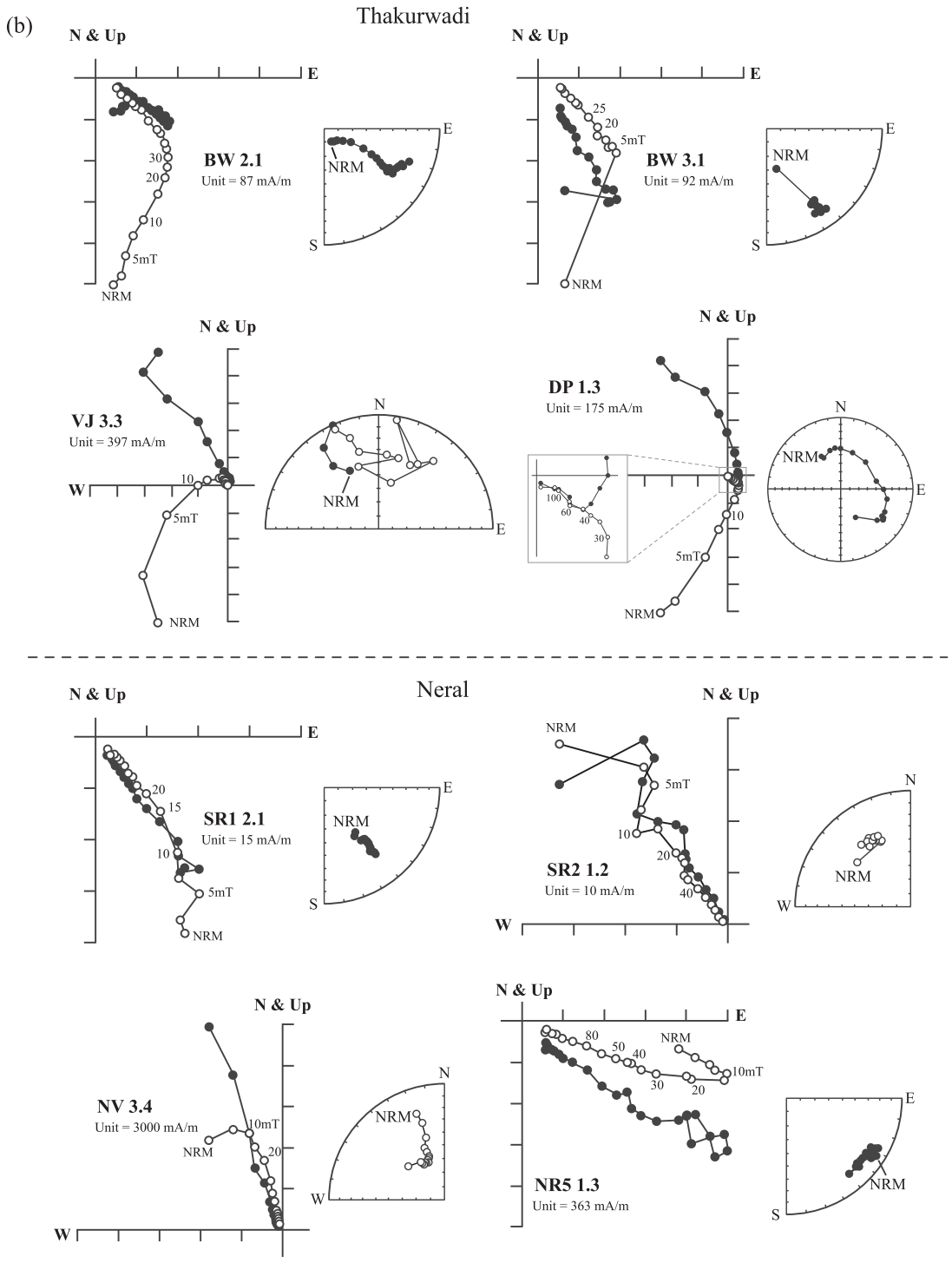

Figure 3. *(Continued.)*

nine VGPs of N-polarity and three VGPs of R-polarity in GI, and eleven VGPs of N-polarity and six VGPs of R-polarity in GII. The corresponding ChRMs of the two groups and their means with 95 per cent confidence circles are shown in Fig. 4(c). The details of the two groups are:

Group I: Nine dykes of N-polarity are: Nos. 2, 5, 7–10, 16, 18 and 21 (Table 3) whose mean direction is at $D_m = 337.8^\circ$, $I_m = -39.4^\circ$ ($k = 130.7$, $\alpha_{95} = 4.5^\circ$, $N = 9$) with a resultant pole located at 43.5°S, 102.6°E ($A_{95} = 4.6^\circ$). Three dykes of R-polarity are: Nos. 25, 28 and 32 whose mean is at $D_m = 150.7^\circ$, $I_m = 44.1^\circ$ ($k = 147.1$, $\alpha_{95} = 10.2^\circ$, $N = 3$) with corresponding pole at 36.6°S, 107.6°E ($A_{95} = 8.9^\circ$; Table 3). Although the number of dykes is small, the mean of normal polarity dykes is antipodal to the mean of reverse polarity dykes. This is obvious from Fig. 4(d) where the 95 per cent confidence circles of the two polarities intersect when one of them is inverted. The pole positions computed above

Table 3. The palaeomagnetic results from 33 dykes along the West Coast and six basement flows near Mumbai.

Site	S. No.	Before tilt correction				*n*	After tilt correction				Φ′(E)	λ′(S)	Gr/Ch
		D	*I*	*κ*	α_{95}		*D*	*I*	*κ*	α_{95}			
BA	1	317.5	−58.2	59.2	6.3	10	303.5	−41.8	59.2	6.3	127.0	20.0	II/31N
BI2	2	341.6	−43.8	303.7	2.8	11	333.5	−38.3	159.6	3.6	107.7	42.2	I/29N
CP1	3	321.0	−53.4	169.0	3.3	12	310.4	−39.5	168.9	3.3	125.4	26.2	II/31N
CP2	4	322.7	−46.0	181.8	4.1	8	314.6	−35.5	181.6	4.1	125.4	30.8	II/31N
KF2	5	349.6	−42.2	85.5	6.0	8	345.9	−40.0	85.6	6.0	93.1	46.2	I/29N
KF3[a]	6	355.3	−41.4	60.9	9.9	5	1.6	−41.6	61.1	9.9	71.6	48.0	
KF4	7	326.4	−50.4	35.0	13.1	5	331.6	−43.5	260.1	4.8	106.9	38.1	I/29N
KL	8	335.9	−58.0	266.7	3.2	9	341.5	−45.3	264.2	3.2	96.0	40.8	I/29N
KS	9	347.6	−37.4	912.5	2.2	6	345.6	−36.4	927.5	4.1	94.6	48.9	I/29N
MJ1	10	329.7	−23.7	60.8	6.2	10	333.9	−28.6	60.3	6.3	113.4	47.5	I/29N
MJ2[a]	-Not Stable-												
MR1	11	322.0	−42.4	51.2	6.4	11	322.0	−42.4	51.2	6.4	115.3	33.6	II/31N
MR2	12	329.3	−52.3	59.9	5.9	11	321.0	−45.4	59.7	6.0	114.1	31.3	II/31N
NR3	13	319.0	−65.2	42.9	7.5	10	311.7	−39.7	42.9	7.5	124.9	26.9	II/31N
NV	14	344.1	−72.9	41.7	9.5	7	296.4	−50.3	29.9	11.2	125.2	11.0	II/31N
SD	15	321.0	−70.6	60.9	6.2	10	300.8	−53.2	60.8	6.2	120.8	12.4	II/31N
SR2	16	323.6	−32.2	78.1	8.7	5	330.7	−38.6	74.6	8.9	110.9	40.2	I/29N
UW	17	350.5	−63.4	204.3	3.9	8	323.7	−51.9	204.3	3.9	108.5	28.2	II/31N
VH1	18	329.2	−37.9	84.1	5.6	9	332.1	−41.2	190.7	3.7	107.1	40.0	I/29N
VH2	19	311.4	−57.7	40.0	8.2	9	313.2	−47.2	40.0	8.2	118.2	24.9	II/31N
VH3	20	320.8	−49.0	68.0	8.2	6	319.9	−47.4	68.0	8.2	114.2	28.9	II/31N
VJ	21	346.2	−40.8	23.8	16.0	5	346.2	−40.8	23.8	16.0	91.6	45.6	I/29N
BI1	22	130.8	51.1	92.7	3.0	23	134.5	50.0	110.9	2.8	115.4	23.8	II/31R
BW	23	117.5	40.5	269.5	2.3	16	122.4	49.2	272.5	2.2	122.4	15.8	II/31R
DP	24	135.3	45.3	21.0	10.2	11	135.3	45.3	21.0	10.2	118.1	26.6	II/31R
KF1	25	142.7	37.2	158.3	2.5	22	149.0	43.8	213.4	1.8	108.1	36.4	I/29R
NR1	26	138.0	65.6	213.9	2.1	22	127.4	54.6	241.0	2.1	116.6	16.5	II/31R
NR2[a]	27	83.1	43.7	61.3	4.6	17	81.7	46.3	61.3	4.6	139.4	−16.4	
NR4	28	142.6	43.4	56.8	4.1	22	147.9	50.4	56.5	4.2	106.3	30.9	I/29R
NR5[a]	29	116.3	14.5	77.2	4.6	14	114.8	27.5	87.7	4.3	141.0	16.9	
PN	30	137.9	60.4	53.7	3.9	26	130.8	49.4	53.7	3.9	118.0	21.8	II/31R
RV	31	129.5	39.2	77.1	3.2	26	129.5	39.2	77.1	3.2	126.0	25.7	II/31R
SR1	32	149.2	32.0	314.8	2.2	14	153.6	37.7	314.5	2.2	108.5	42.4	I/29R
Mean dyke (9 dykes–29N)		}Group I					**337.8**	**−39.4**	**130.7**	**4.5**	**102.6**	**43.5**	A_{95} **= 4.6**
Mean dyke (3 dykes–29R)							**150.7**	**44.1**	**147.1**	**10.2**	**107.6**	**36.6**	A_{95} **= 8.9**
Mean dyke (11 dykes–31N)		}Group II					**312.6**	**−45.2**	**93.3**	**4.8**	**120.1**	**25.0**	A_{95} **= 5.3**
Mean dyke (6 dykes–31R)							**130.1**	**48.0**	**176.8**	**5.1**	**119.1**	**22.2**	A_{95} **= 5.2**
Flows													
RVF		126	53	72	6.6	13					117	16	
KF1F		123	55	135	6.9	13					118	14	
PNF1		130	42	53	7.7	12					124	25	
PNF2		132	43	77	6.4	10					122	26	
BWF		133	44	220	6.2	10					120	26	
DPF		122	44	281	4.6	10					126	18	
Mean (*N*= 6)		**128**	**47**	**156**	**5.4**	**68**					**121**	**21**	A_{95} **= 5.3**

[a]Not included in calculation of means; *n*, number of specimens yielding stable vectors; *N*, number of dykes/flows; *D* and *I*, declination and inclination (in degrees) of ChRM vectors; *κ*, precision parameter for directions; α_{95}, radius of 95 per cent confidence cone for mean directions; A_{95}, radius of the 95 per cent confidence cone for VGPs; λ′and Φ′, latitude and longitude of mean VGP; Gr/Ch, Group/Chron.

appear on the younger segment of the APWP (Fig. 5c) where they are designated as C29N/C29R corresponding to Normal/Reverse polarity mean.

Group II: Eleven dykes of N-polarity in this group are Nos. 1, 3–4, 11–15, 17, 19–20, and six dykes of R-polarity are Nos. 22–24, 26 and 30–31 (Table 3). The overall mean of 11 N-dykes is at $D_m = 312.6°, I_m = -45.2°$ ($k = 93.3, \alpha_{95} = 4.8°, N = 11$) with corresponding pole (C31N) located at 25° S, 120.1° E ($A_{95} = 5.3°$), while the combined mean of six R-dykes is at $D_m = 130.1°$, $I_m = 48.0°$ ($k = 176.8$, $\alpha_{95} = 5.1°$, $N = 6$ sites) with a resultant pole (R GII dykes) located at 22.2°S, 119.1°E ($A_{95} = 5.2°$). These pole positions occur on the older segment of the APWP (Fig. 5c). Six R-flows associated with GII dykes have been grouped separately and the corresponding pole (21°S, 121°E, $A_{95} = 5.3°$) occurs on the older segment of APWP, very close to R GII dykes pole. In the reversal test, $\gamma_o = 6.3°$ and $\gamma_c = 9.1°$ for GI dykes, while GII shows $\gamma_o = 2.9°$ and $\gamma_c = 9.1°$, indicating a positive reversal test of type B (McFadden & McElhinny 1990). We like to point out at this point that, given fewer numbers of dykes, some bias may have been introduced in this statistical result, and so, this result

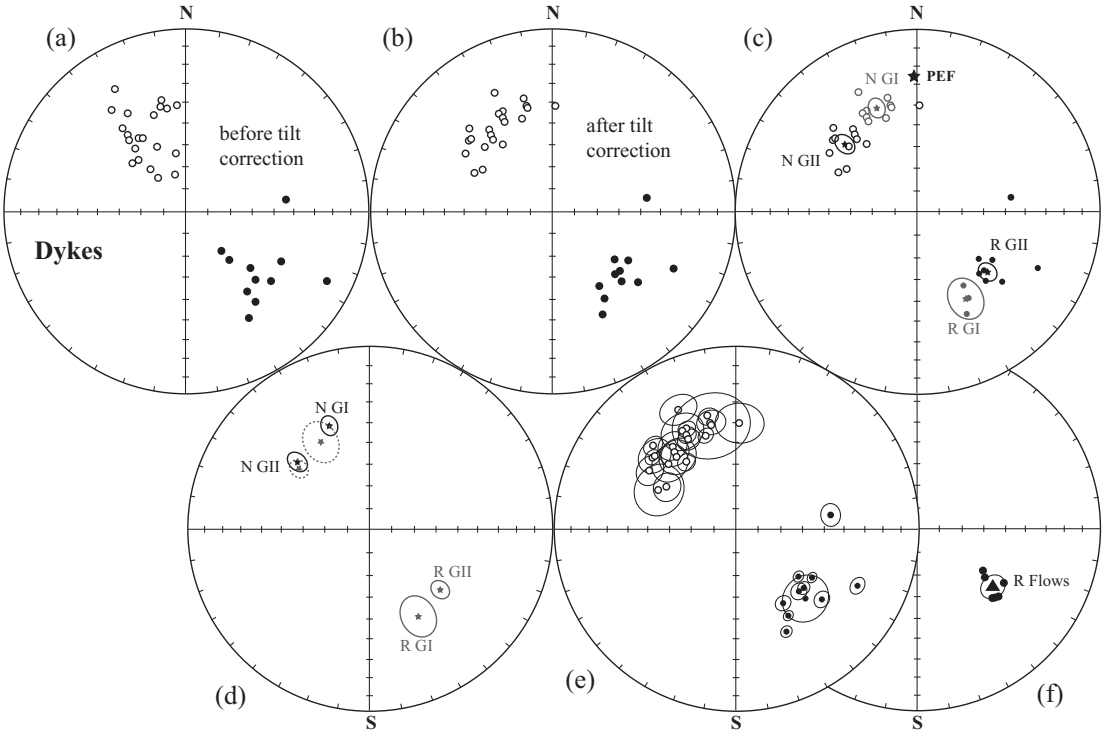

Figure 4. Equal area projections of dyke (site) mean directions for normal (open circles) and reverse (solid circles) polarity dykes. (a) before tilt correction; (b) after tilt correction; (c) Group I (N GI, R GI) and Group II (N GII, R GII) dyke means identified in the tilt corrected means with their α_{95} circles. PEF is present-day Earth's field; (d) Group I and Group II means with reverse polarity means inverted to show that α_{95} circles of the N and R polarities in the respective groups intersect; (e) dyke means with their individual α_{95} circles indicating the drifting of the geomagnetic field while the dykes acquired their stable magnetization and (f) mean directions of flows and solid triangle is the combined mean for flows with α_{95} circle.

needs to be substantiated by further investigation of larger number of dykes.

4.2.4 Averaging of palaeosecular variation

It is pertinent at this point to examine whether or not palaeosecular variation (PSV) has been adequately sampled in the two groups of ChRMs identified in this study. Towards this end, we have calculated the angular dispersion (S_b) of VGPs based on the expressions given by Johnson *et al.* (2008) and Biggin *et al.* (2008). The calculation is based on combining the N-and R-polarity site (dyke) means in each group by inverting the R-Polarity means. This gives 12 (9 + 3) sites for GI and 17 (11 + 6) sites for GII for computing S_b. Values of S_b so obtained are 11.2 for GI and 20.8 for GII. Compared to a well estimated value of ∼13 for Deccan palaeolatitudes (McFadden & McElhinny 1984; McFadden *et al.* 1991) required for inferring about adequate sampling of secular variation, our calculated value of S_b is a little lower for GI and significantly higher for GII. A possible reason for the incompatibility of our calculated values with the standard one may be the inadequate data points for statistical analysis.

We like to point out here that in the computation of DSP (Vandamme *et al.* 1991) also, a large angular dispersion (∼17.4) was observed between sites. Thus, under the obvious limitation of smaller number of sites (dykes), we believe that the statistical consideration does not negate the averaging of PSV in our present data. Furthermore, the occurrence of both polarities in the two groups with mean of N-polarity ChRMs antipodal to the mean of R-polarity ChRMs is another evidence of PSV averaging. Adequate averaging of PSV in the present data seems to be further reinforced qualitatively by the cross-cutting relationship of the dykes observed in the field—where among two sets of cross-cutting dykes (BI1–BI2 Borlai and KF1–KF2 Korlai Fort) and one set of N–S trending co-existed dykes at Sireva across Ulhas River (Fig. 1 and Table 1), older ones were found to be reversely magnetized and younger ones exhibited normal magnetization.

5 DISCUSSION

The consistency of magnetization with no evidence of magnetic overprinting in the isolated stable component of magnetization together with tilt correction and positive reversal test indicates that ChRM directions are free from secondary NRM components and hence, probably primary and closely associated with the emplacement of dykes. Also, as demonstrated above, the palaeomagnetic data have adequately averaged PSV. Thus the pole positions computed for the two groups of dykes, GI and GII, truly represent the geomagnetic field at the time dykes acquired their magnetization. On the other hand, palaeomagnetic results from the flow samples collected at the base of the Traps around the Mumbai coastal region also reveal a reverse magnetization (Fig. 4f) which is not significantly different from R-polarity magnetization of GII dykes (Figs 4c and d), implying thereby no significant difference in their emplacement ages.

Figs 5c–e depict pole positions obtained in this study along with other reported poles from flows and dykes of the DVP on three different APWPs—one reported by Klootwijk & Peirce (1979) and the others by Besse & Courtillot (2002) and Torsvik & Van der Voo (2002). The occurrence of GI poles in close proximity of the DSP on all the three APWPs clearly suggests an age corresponding to

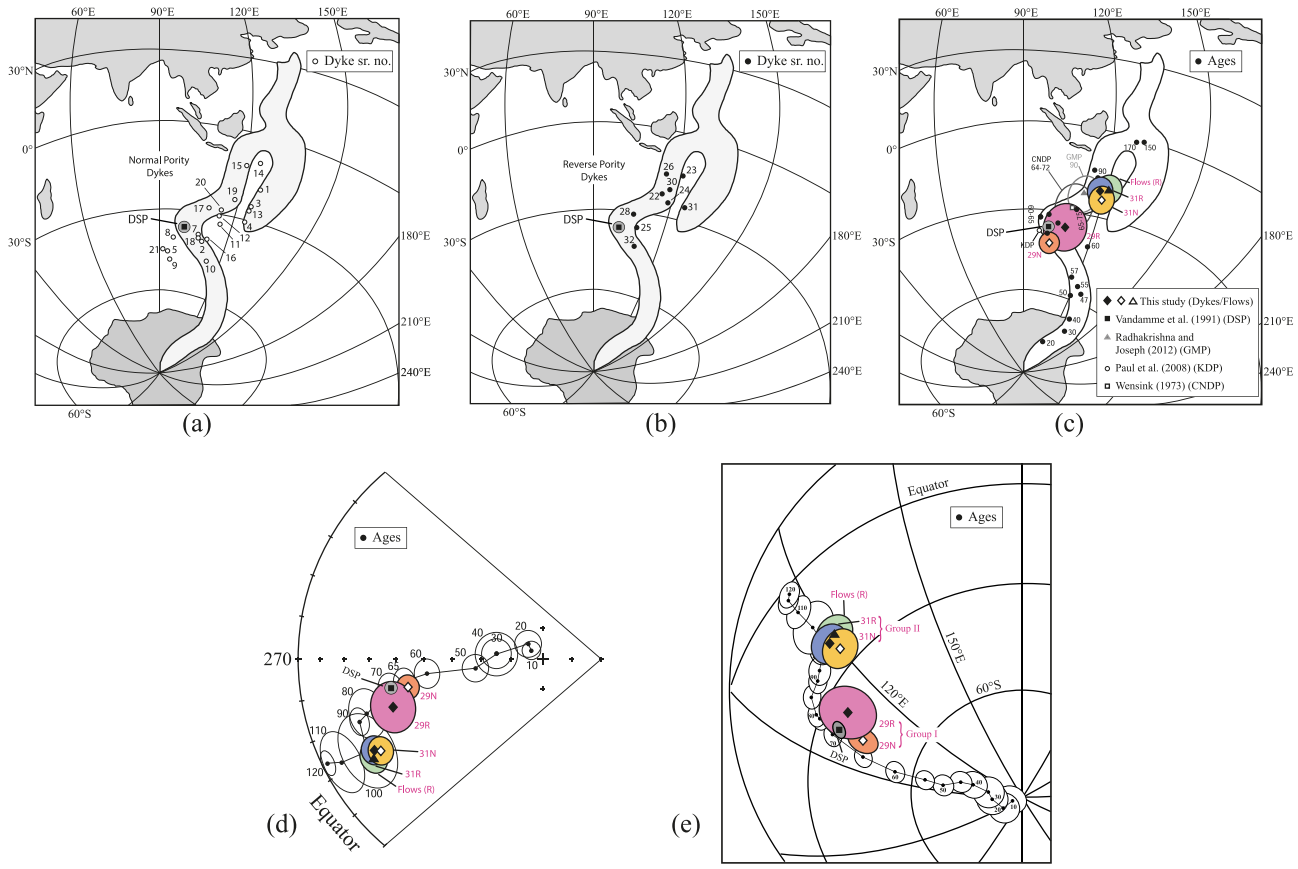

Figure 5. Plot of VGPs and pole positions on the Indian APWP. (a) VGPs of dykes with normal magnetic polarity and (b) VGPs of dykes with reverse magnetic polarity. Both plots are on the APWP of Klootwijk and Peirce (KP 1979). DSP is the Deccan Superpole (Vandamme *et al.* 1991). Numbers in the Figures are the dyke numbers as specified in Table 3. Pole positions computed for the dykes and flows in the present study plotted on three APWPs (c–e) favoured by different authors along with some other reported palaeopoles. (c) Palaeopoles plot on the APWP of KP 1979; (d) Palaeopoles plot on the APWP of Besse & Courtillot (BC 2002) and (e) Palaeopoles plot on the APWP of Torsvik & Van der Voo (TV 2002). Ages with uncertainty ellipses are indicated in Ma for different segments of the APWP. The time window duration is 10 Ma for BC 2002 and 5 Ma for TV 2002. In inset in panel (c) are listed the authors' names and their respective pole positions plotted on the APWP.

the DSP (65.5 ± 3 Ma, Vandamme *et al.* 1991), or the date for K–Pg boundary (66.043 ± 0.086 Ma, Renne *et al.* 2015; Shcoene *et al.* 2015). Accordingly, the N- and R-polarity magnetizations of GI dykes may correspond to Chrons 29N (~64.43–65.52 Ma) and 29R (~65.52–66.50 Ma) respectively which constitute part of DSP computation from the palaeomagnetic results of flows (Vandamme *et al.* 1991). The inclusion of N-polarity magnetization of GI in Chron 29N (and not 30N of the DSP) seems to be justified by the availability of radiometric date of one of the lamprophyre dykes of GI (Dyke MJ1, pole no. 10, Fig. 5a) which has Rb–Sr date of *ca.* 64.9 ± 0.8 Ma (Sahu *et al.* 2003). Additionally, majority of GI poles were collected from the coastal dyke swarm, which Vanderkluysen *et al.* (2011) attributed to post-Deccan Seychelles rifting at ~62 Ma based on geochemistry.

Furthermore, the current consensus is that the entire southern Konkan succession belonging to Wai subgroup is 29R (see Fig. 1a). The lava succession through which N-dykes cut along the Alibag–Murud section was probably the Konkan succession that has already been established as reverse (Chron 29R) by previous workers. Thus the recorded normal signature, 29N is younger than the bulk of the eruption, and which places the emplacement of these N-dykes post 29R. In contrast, the magnetization corresponding to R-dykes of GI cutting through Wai subgroup units (Poladpur–Ambenali Fms, Fig. 1a) was perhaps acquired during C29R, which is consistent with palaeomagnetic and radiometric dating *ca.* 66–65 Ma for the vast bulk of the Deccan succession (Renne *et al.* 2015; Schoene *et al.* 2015).

The GII dyke poles, on the other hand, and the pole from R-polarity mean flow directions appear to be significantly displaced from the DSP towards the older segment of the APWP. This indicates an older period of emplacement than GI dykes. On the APWP (Fig. 5c) of Klootwijk & Peirce (1979), these poles fall close to *ca.* 75–80 Ma pole, and *ca.* 64–72 Ma pole computed by Wensink (1973) from the combined lower flows at Nagpur. These poles are also seen to be not far away from Grand Mean Pole (GMP, 90 Ma) from the Karnataka–Kerala dykes (Radhakrishna & Joseph 2012). However, on both the synthetic APWPs (Figs 5d and e), GII poles fall precisely at 100 Ma between the windows of 90–110 Ma, in apparent discordance with their location on the other APWP (Fig. 5c).

While we are unable to explain this discrepancy between the synthetic APWPs on the one hand and the APWP based on the real age data of Klootwijk & Peirce (1979) on the other, we like to mention that most of the interpretations of palaeomagnetic results in the development of Deccan flow magnetostratigraphy have been done with reference to the APWP of Klootwijk & Peirce (1979). We, therefore, prefer to stand by the older APWP. This stand seems to be justified, also from the location of GII poles on the synthetic APWPs

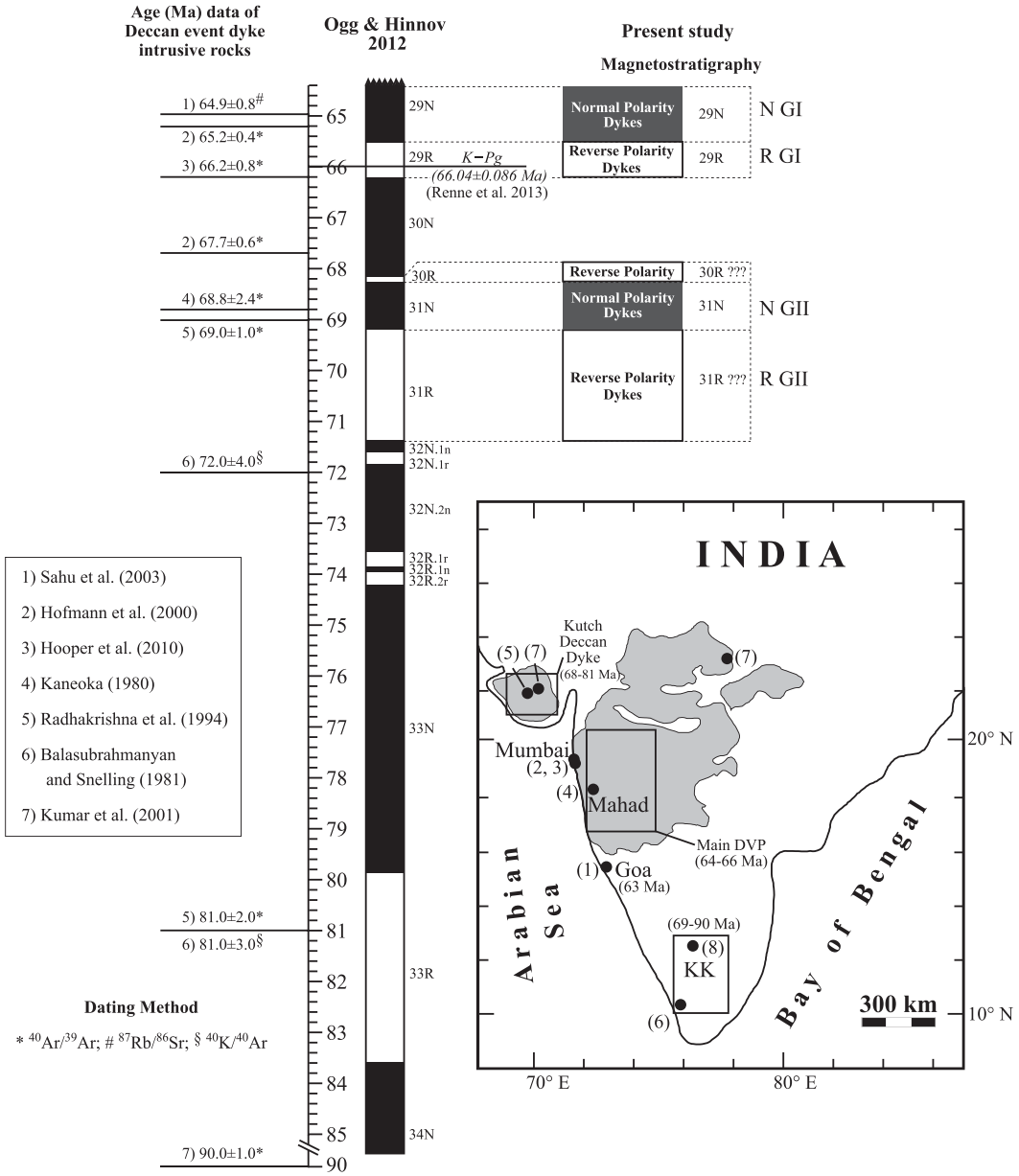

Figure 6. Comparison between published radiometric ages of West Coast Deccan event dykes and predicted ages determined from this study by magnetostratigraphic correlation of normal and reverse polarity dykes to Group I Chrons (29N, 29R) and Group II Chrons (31N, 30R or 31R) of the geomagnetic polarity timescale of Ogg & Hinnov (2012). Cretaceous/Palaeogene (K–Pg) boundary age of 66.04 ± 0.086 Ma (Renne *et al.* 2013) is shown by the solid line. Abbreviations in the India map are: KK, Konkan–Kerala dykes and DVP, Deccan Volcanic Province dykes.

which cannot be reconciled with the geochronological data from the DVP. However, irrespective of whatever has been argued above, we notice that whichever APWP we may choose, there appears compelling evidence that GII poles represent a magnetic signature of an older episode of the Deccan effusion. But, in the absence of radiometric dates from the dykes of this group, and based on palaeomagnetic results alone, we cannot conclusively assign an age of magnetization. Nevertheless, some inferences can be drawn regarding a probable time of magnetization from the present palaeomagnetic data in conjunction with some previously reported geochronological studies of the Deccan flow sequence and dykes.

The published radiometric dates from the flows (e.g. Besse *et al.* 1986; Venkatesan *et al.* 1986; Baksi 1987; Courtillot *et al.* 1988; Duncan & Pyle 1988; Pande 2002; Pande *et al.* 2004; Chenet *et al.* 2009; Baksi 2014; Renne *et al.* 2015; Schoene *et al.* 2015), the dykes of DVP in the present study area (e.g. Hofmann *et al.* 2000; Sahu *et al.* 2003; Hooper *et al.* 2010), and Deccan-age dykes in the Kutch (e.g. Kaneoka 1980; Balasubrahmanyan & Snelling 1981) and southern India (e.g. Radhakrishna *et al.* 1994) have a spread in ages that cover magnetic Chrons 29N to 32R on the GPTS of Ogg & Hinnov (2012; Fig. 6). Also, based on the GPTS of Ogg & Smith (2004), Collier *et al.* (2008) divided the Deccan volcanic record into three stages: pre-Deccan (~78–67 Ma, 33N–30N), Deccan (~67–63 Ma, 30N–27R) and post-Deccan (~63–58 Ma, 27N–26 N). In the light of above geochronological reports in respect of magnetochrons covered by the Deccan volcanic outflow and the obvious location of the palaeopoles on the APWP, we are inclined to assign Chrons 31N (~68.30–69.25 Ma) for the N-polarity pole, and either Chron 30R

(∼68.20–68.30 Ma) or 31R (∼69.25–71.35 Ma) for the R-polarity pole from GII dykes (Fig. 6). Similarly, the reverse polarity pole corresponding to mean flow direction may also be placed along with GII R-poles. Our choice of Chrons 31N and 30R (or 31R) for GII dykes is not incompatible with the radiometric age data, because these are the closest Chrons on the older side of the already established three-Chron N–R–N magnetostratigraphy.

We like to mention here that our inference on the age of GII dykes is not consistent with the dates of the stratigraphic units which the dykes cut through or the dates of dykes (other than those used in this study) available from our study area. It seems likely that the GII dykes cut flows of either upper Wai sub-group units or the lower part of either Kalsubai or Lonavala and include from older to younger—Neral, Thakurwadi, Khandala and Poladpur Fms in the main succession (Fig. 1a). Even though all of these units have been well-constrained by $^{40}Ar/^{39}Ar$ and U/Pb dates (range of dates *ca.* 62–67 Ma), it seems a serious challenging task to use a reasonable maximum age timeframe in which to place the normal and Chrons of reverse polarity identified by our palaeomagnetic results. Therefore, in the face of such discordance, more thorough sampling, palaeomagnetic, and geochronological data on the basement Deccan flows and dykes are needed to conclusively establish the age of magnetization as inferred from the palaeomagnetic findings of this study. However, based on the present study, we have provided palaeomagnetic interpretation of our results in Fig. 6 regarding the time of emplacement of GII dykes corresponding to Chrons 31N, 30R (or 31R).

At this point, we like to invoke two major episodes of continental breakup that took place along the western continental margin of India during the Cretaceous involving the breakup of Greater India (India and Seychelles) from the Madagascar at ∼88 Ma (e.g. Storey *et al.* 1995; Pande *et al.* 2001; Bhattacharya & Yatheesh 2015), and subsequently the breakup of Indian subcontinent and the Seychelles at ∼62 Ma post main phase Deccan volcanism (e.g. Collier *et al.* 2008). The latter episode is contemporaneous with the minor volcanism (Collier *et al.* 2008; Vanderkluysen *et al.* 2011). Also, we note that dolerite dykes in southern India (Fig. 6) have an identical age to St. Mary's island rhyolites (Radhakrishna *et al.* 1994; Kumar *et al.* 2001) and basic units in Madagascar (Storey *et al.* 1995), but no correlations have been established so far. However, it seems quite possible that the dykes under the present study were emplaced within the eruption of the Deccan Traps during the 64.9 Ma that is the radiometric date of N GI dyke (MJ1) and the ∼71.35 Ma suggested APWP-GPTS2012 date for R GII dykes (Fig. 6). This may be as early as India–Madagascar breakup at ∼88 Ma, and continued till the onset of India–Seychelles breakup at ∼62 Ma, the two major tectonic events witnessed by the western continental margin of India. Further, following Torsvik *et al.* (2000) and Radhakrishna & Joseph (2012), the ∼85–91 Ma volcanics are considered to be associated with the Marion Hotspot activity, that was instrumental for India–Madagascar breakup and the ∼65–70 Ma volcanics are related with Reunion Hotspot.

In conclusion, the present investigation appears to lay bare the presence of two more magnetic reversals, 31N and 30R or (31R?) in the Deccan volcanic sequence in addition to the widely accepted only three-Chron (30N–29R–29N) magnetostratigraphy. Chennet *et al*. (2008, 2009) argued for the existence of a smaller short peak of activity at C30R, then a long period of quiescence until the main event in C29R, which was questioned by the recent geochronology (Renne *et al.* 2015; Schoene *et al.* 2015). This is the first time that stable magnetization of both N- and R-polarity has been isolated from the dykes in the basement of Deccan sequence, indicating that the main succession inland of Mumbai represents prolonged and sporadic eruption during the Deccan phase. Thus, contrary to the earlier view of no significant APW during Deccan volcanism, the present result does exhibit an APW, albeit small, during the intrusion of the dykes under this study. The angular displacement between mean directions of the younger GI and older GII dykes is ∼20° (Fig. 5) and the corresponding palaeolatitude differs by ∼4.4°. Since the age of GII dykes cannot be constrained under the present state of available data, it is not possible to deduce a velocity for the northward movement of Indian plate during the acquisition of GI and GII magnetization by the dykes of DVP.

ACKNOWLEDGEMENTS

We thank A. Biggin and E. Petrovsky for the editorial advice and all anonymous reviewers for invaluable suggestions that have contributed to rework at the field sampling, experimental work and analysis of data that improved the contents and discussion of this manuscript. We are grateful to B.V. Lakshmi, Md. Arif, Prasanta Kumar Das and Saumitra Misra for participating in the field work. A special thanks to S.P. Prizomwala for working with us on recent geological field work for estimating tilting of Deccan dykes and making it believable.

REFERENCES

Auden, J.B., 1949. Dykes in western India—a discussion of their relationships with the Deccan Traps, *Trans. Nat. Inst. Sci. India,* **3,** 123–157.

Baksi, A.K., 1987. Critical evaluation of the age of the Deccan Traps, India: implications for flood-basalt volcanism and faunal extinctions, *Geology,* **15**(2), 147–150.

Baksi, A.K., 2014. The Deccan Trap – Cretaceous–Paleogene boundary connection; new $^{40}Ar/^{39}Ar$ ages and critical assessment of existing argon data pertinent to this hypothesis, *J. Asian Earth Sci.,* **84,** 9–23.

Baksi, A.K., Archibald, D.A. & Farrar, E., 1996. Intercalibration of 40Ar39Ar dating standards, *Chem. Geol.,* **129**(3–4), 307–324.

Balasubrahmanyan, M.N. & Snelling, N.J., 1981. Extraneous argon in lavas and dykes of the Deccan Volcanic Province, *Geol. Soc. India Mem.,* **3,** 259−264.

Basavaiah, N., 2011. *Geomagnetism: Solid Earth and Upper Atmosphere Perspectives,* Springer, Netherlands.

Basavaiah, N. & Khadkikar, A.S., 2004. Environmental magnetism and its application towards paleomonsoon reconstruction, *J. India Geophys. Uni.,* **8**(1), 1–14.

Basavaiah, N., Appel, E., Lakshmi, B.V., Deenadayalan, K., Satyanarayana, K.V.V., Misra, S., Juyal, N. & Malik, M.A., 2010. Revised magnetostratigraphy and characteristics of the fluviolacustrine sedimentation of the Kashmir basin, India, during Pliocene-Pleistocene, *J. geophys. Res.,* **115**(B8), B08105, doi: 10.1029/2009JB006858.

Basavaiah, N., Mahesh Babu, J.L.V., Gawali, P.B., Naga Kumar, K.Ch.V., Demudu, G., Prizomwala, S.P., Hanamgond, P.T. & Nageswara Rao, K., 2015. Late Quaternary environmental and sea level changes from Kolleru Lake, SE India: inferences from mineral magnetic, geochemical and textural analyses, *Quat. Int.,* **371,** 197–208.

Beane, J.E., Turner, C.A., Hooper, P.R., Subbarao, K.V. & Walsh, J.N., 1986. Stratigraphy, composition and form of the Deccan basalts, Western Ghats, India, *Bull. Volcanol.,* **48**(1), 61–83.

Besse, J. & Courtillot, V., 2002. Apparent and true polar wander and the geometry of the geomagnetic field in the last 200 Myr, *J. geophys. Res.,* **B107,** 2300, doi:10.1029/ 2000JB000050.

Besse, J. *et al.*, 1986. The Deccan Traps (India) and Cretaceous-Tertiary boundary events, in *Global Bio-Events*, Lecture Notes in Earth Sciences, Vol. 8, pp. 365–370, ed. Walliser, O.H., Springer.

Bhattacharya, G.C. & Yatheesh, V., 2015. Plate-tectonic evolution of the deep ocean basins adjoining the western continental margin of India—a

proposed model for the early opening scenario, in *Petroleum Geoscience: Indian Contexts*, pp. 1–61, ed. Mukherjee, S., Springer.

Bhattacharji, S., Chatterjee, N., Wampler, J.M., Nayak, P.N. & Deshmukh, S.S., 1996. Indian intraplate and continental margin rifting, lithospheric extension, and mantle upwelling in Deccan flood basalt volcanism near the K/T boundary: evidence from Mafic dike swarms, *J. Geol.,* **104**(4), 379–398.

Biggin, A., van Hinsbergen, D.J.J., Langereis, C.G., Straathof, G.B. & Deenen, M.H., 2008. Geomagnetic secular variation in the Cretaceous Normal Superchron and in the Jurassic, *Phys. Earth planet. Inter.,* **169**(1-4), 3–19.

Biswas, S.K., 1987. Regional tectonic framework, structure and evolution of the western marginal basins of India, *Tectonophysics,* **135**(4), 307–327.

Campbell, I.H., 1998. The mantle's chemical structure; insights from the melting products of mantle plumes, in *The Earth's Mantle; Composition, Structure, and Evolution*, pp. 259–310, ed. Jackson, I., Cambridge Univ. Press.

Campbell, I.H., 2005. Large igneous provinces and the mantle plume hypothesis, *Elements,* **1**(5), 265–269.

Campbell, I.H. & Griffiths, R.W., 1990. Implications of mantle plume structure for the evolution of flood basalts, *Earth planet. Sci. Lett.,* **99**(1-2), 79–93.

Chenet, A.L., Quidelleur, X., Fluteau, F., Courtillot, V. & Bajpai, S., 2007. ^{40}K–^{40}Ar dating of the Main Deccan large igneous province: further evidence of KTB age and short duration, *Earth planet. Sci. Lett.,* **263**(1-2), 1–15.

Chenet, A.L., Fluteau, F., Courtillot, V., Gerard, M. & Subbarao, K.V., 2008. Determination of rapid Deccan eruptions across the Cretaceous-Tertiary boundary using paleomagnetic secular variation: Results from a 1200-m-thick section in the Mahabaleshwar escarpment, *J. geophys. Res.,* **113**(B4), B04101, doi:10.1029/2006JB004635.

Chenet, A.L., Courtillot, V., Fluteau, F., Gerard, M., Quidelleur, X., Khadri, S.F.R., Subbarao, K.V. & Thordarson, T., 2009. Determination of rapid Deccan eruptions across the Cretaceous-Tertiary boundary using paleomagnetic secular variation: 2. Constraints from analysis of eight new sections and synthesis for a 3500-m-thick composite section, *J. geophys. Res.,* **114**(B6), B06103, doi:10.1029/2008JB005644.

Church, N., Feinberg, J. & Harrison, R., 2011. Low-temperature domain wall pinning in titanomagnetite: quantitative modeling of multidomain first-order reversal curve diagrams and AC susceptibility, *Geochem. Geophys. Geosyst.,* **12**(7), doi:10.1029/2011GC003538.

Collier, J.S., Sansom, V., Ishizuka, O., Taylor, R.N., Minshull, T.A. & Whitmarsh, R.B., 2008. Age of Seychelles–India break-up, *Earth planet. Sci. Lett.,* **272**(1-2), 264–277.

Courtillot, V., Besse, J., Vandamme, D., Montigny, R., Jaeger, J.J. & Cappetta, H., 1986. Deccan flood basalts at the Cretaceous/Tertiary boundary?, *Earth planet. Sci. Lett.,* **80**(3-4), 361–374.

Courtillot, V., Feraud, G., Maluski, H., Vandamme, D., Moreau, M.G. & Besse, J., 1988. Deccan flood basalts and the cretaceous/Tertiary boundary, *Nature,* **333**(6176), 843–846.

Courtillot, V., Davaille, A., Besse, J. & Stock, J.M., 2003. Three distinct types of hotspots in the Earth's mantle, *Earth planet. Sci. Lett.,* **205**(3-4), 295–308.

Courtillot, V., Gallet, Y., Rocchia, R., Feraud, G., Robin, E., Hoffman, C., Bhandari, N. & Ghevariya, Z.G., 2000. Cosmic markers, 40Ar/39Ar dating and paleomagnetism of the KT sections in the Anjar area of the Deccan large igneous province, *Earth planet. Sci. Lett.,* **182**(2), 137–156.

Day, R., Fuller, M.D. & Schmidt, V.A., 1977. Hysteresis properties of titanomagnetites: Grain-size and compositional dependence, *Phys. Earth planet. Inter.,* **13**(4), 260–267.

Deshmukh, S.S. & Sehgal, M.N., 1988. Mafic dyke swarms in Deccan Volcanic Province of Madhya Pradesh and Maharashtra, *Mem. Geol. Soc. India,* **10,** 323–340.

Dessai, A.G. & Bertrand, H., 1995. The "Panvel Flexure" along the Western Indian continental margin: an extensional fault structure related to Deccan magmatism, *Tectonophysics,* **241**(1-2), 165–178.

Dessai, A.G. & Viegas, A.A.A.A., 1995. Multi-generation mafic dyke swarm related to Deccan magmatism, South of Bombay: Implications on the evolution of the western Indian continental margin, in *Dyke Swarms of Peninsular India,* Vol. 33, pp. 435–451, ed. Devaraju, T.C., Mem. Geol. Soc. India.

Dessai, A.G., Rock, N.M.S., Griffin, B.J. & Gupta, D., 1990. Mineralogy and petrology of some xenolith-bearing alkaline dykes associated with Deccan magmatism, south of Bombay, India, *Eur. J. Mineral.,* **2**(5), 667–686.

Deutsch, E.R., Radhakrishnamurty, C. & Sahasrabudhe, P.W., 1959. Paleomagnetism of the Deccan Traps, *Ann. Geophys.,* **15,** 39–59.

Devey, C.W. & Lightfoot, P.C., 1986. Volcanological and tectonic control of stratigraphy and structure in the western Deccan Traps, *Bull. Volcanol.,* **48**(4), 195–207.

Duncan, R.A. & Pyle, D.G., 1988. Rapid eruption of the Deccan flood basalts at the Cretaceous/Tertiary boundary, *Nature,* **888**(6176), 841–843.

Dunlop, D.J., 2002. Theory and application of Day plot (M_{rs}/M_s versus H_{cr}/H_c) 2. Application to data for rocks, sediments, and soils, *J. geophys. Res.,* **107,** B3, doi:10.1029/2001JB000487.

Enkin, R.J., 2003. The direction–correction tilt test: an all-purpose tilt/fold test for paleomagnetic studies, *Earth planet. Sci. Lett.,* **212**(1-2), 151–166.

Ernst, R.E. & Buchan, K.L., 2003. Recognizing mantle plumes in the geological record, *Annu. Rev. Earth Planet. Sci.,* **31**(1), 469–523.

Fisher, R.A., 1953. Dispersion on a sphere, *Proc. R. Soc. A,* **A217**(1130), 295–305.

Gallet, Y., Weeks, R., Vandamme, D. & Courtillot, V., 1989. Duration of Deccan trap volcanism: a statistical approach, *Earth planet. Sci. Lett.,* **93**(2), 273–282.

Hofmann, C., Feraud, G. & Courtillot, V., 2000. ^{40}Ar/^{39}Ar dating of mineral separates and whole rocks from the Western Ghats lava pile: further constraints on duration and age of the Deccan traps, *Earth planet. Sci. Lett.,* **180**(1-2), 13–27.

Hooper, P., 1990. The timing of crustal extension and the eruption of continental flood basalts, *Nature,* **345**(6272), 246–249.

Hooper, P., Widdowson, M. & Simon, K., 2010. Tectonic setting and timing of the final Deccan flood basalt eruptions, *Geology,* **39**(9), 839–842.

Jay, A.E. & Widdowson, M., 2008. Stratigraphy, structure and volcanology of the SE Deccan continental flood basalt province: implications for eruptive extent and volumes, *J. Geol. Soc.,* **165**(1), 177–188.

Jay, A.E., Conall, M.N., Widdowson, M., Stephen, S. & Turner, W., 2009. New palaeomagnetic data from the Mahabaleshwar Plateau, Deccan flood basalt province, India: implications for the volcanostratigraphic architecture of continental flood basalt provinces, *J. Geol. Soc.,* **166**(1), 13–24.

Jerram, D.A. & Widdowson, M., 2005. The anatomy of continental flood basalt provinces: geological constraints on the processes and products of flood volcanism, *Lithos,* **79**(3-4), 385–405.

Johnson, C.L. *et al.*, 2008. Recent investigations of the 0-5 Ma geomagnetic field recorded by lava flows, *Geochem. Geophys. Geosyst.,* **9**(4), doi:10.1029/2007GC001696.

Kaneoka, I., 1980. 40Ar/39Ar dating on volcanic rocks of the Deccan traps, India, *Earth planet. Sci. Lett.,* **46**(2), 233–243.

Keller, G., Adatte, T., Gardin, S., Bartolini, A. & Bajpai, S., 2008. Main Deccan volcanism phase ends near the K–T boundary: Evidence from the Krishna–Godavari Basin, SE India, *Earth planet. Sci. Lett.,* **268**(3-4), 293–311.

Kirschvink, J.L., 1980. The least-squares line and plane and the analysis of palaeomagnetic data, *Geophys. J. Int.,* **62**(3), 699–718.

Klootwijk, C.T. & Peirce, J.W., 1979. India's and Australia's pole path since the late Mesozoic and the India–Asia collision, *Nature,* **282**(5739), 605–607.

Knight, K.B., Barker, J.A., Basu, A.R., Dessari, A.G., Renne, P.R. & Waight, T.E., 2000. A question of timing: chronological and isotopic evidence of the Deccan plume, India, in *Penrose Conference 2000 on Volcanic Rifted Margins*, Geological Society of America & Royal Holloway, University of London, Abstract Volume, pp. 43–44.

Kumar, A, Pande, K., Venkatesan, T.R. & Bhaskar Rao, Y.J., 2001. The Karnataka Late Cretaceous dykes as products of the Marion hot spot at the Madagascar-India breakup event: evidence from ^{40}Ar–^{39}Ar geochronology and geochemistry, *Geophys. Res. Lett.,* **28**(14), 2715–2718.

Mahoney, J.J., Duncan, R.A., Khan, W., Gnos, E. & Mc-Cormick, G.R., 2002. Cretaceous volcanic rocks of the South Tethyan suture zone, Pakistan: implications for the Réunion hotspot and Deccan Traps, *Earth planet. Sci. Lett.,* **203**(1), 295–310.

McElhinny, M.W., 1964. Statistical significance of the fold test in palaeomagnetism, *Geophys. J. R. astr. Soc.,* **8**(3), 338–340.

McFadden, P.L. & Jones, D.L., 1981. The fold test in palaeomagnetism, *Geophys. J. Int.,* **61**(1), 53–58.

McFadden, P.L. & McElhinny, M.W., 1984. A physical model for palaeosecular variation, *Geophys. J. Int.,* **78**(3), 809–830.

McFadden, P.L. & McElhinny, M.W., 1990. Classification of the reversal test in palaeomagnetism, *Geophys. J. Int.,* **103**(3), 725–729.

McFadden, P.L., Merrill, R.T., McElhinny, M.W. & Lee, S., 1991. Reversals of the Earth's magnetic field and temporal variations of the dynamo families, *J. geophys. Res.,* **B96**(B3), 3923–3933.

Melluso, L., Sethna, S. F., Morra, V., Khateeb, A. & Javeri, P., 1999. Petrology of the mafic dyke swarm of the Tapti River in the Nandurbar area (Deccan volcanic province), in *Deccan Flood Basalts,* Vol. 10, pp. 735–755, ed. Subbarao, K.V., Mem. Geol. Soc. India.

Melluso, L., Sethna, S.F., D'Antonio, M., Javeri, P. & Bennio, L., 2002. Geochemistry and petrogenesis of sodic and potassic mafic alkaline rocks in the Deccan Volcanic Province, Mumbai Area (India), *Mineral. Petrol.,* **74**(2-4), 323–342.

Mitchell, C. & Widdowson, M., 1991. A geological map of the southern Deccan Traps, India and its structural implications, *J. Geol. Soc.,* **148**(3), 495–505.

Moskowitz, B.M., Jackson, M. & Kissel, C. 1998. Low-temperature magnetic behavior of titanomagnetites, *Earth planet. Sci. Lett.,* **157**(3-4), 141–149.

Ogg, J.G. & Hinnov, L.A., 2012. Cretaceous, in *The Geological Time Scale 2012*, pp. 793–853, eds Ogg, F.M., Schmitz, M.D. & Ogg, G.M., Elsevier.

Ogg, J.G. & Smith, A.G., 2004. The geomagnetic polarity time scale, in *A Geologic Time Scale 2004*, pp. 63–86, eds Gradstein, F.M., Ogg, J.G. & Smith, A.G., Cambridge Univ. Press.

Ozdemir, O., Dunlop, D.J. & Moskowitz, B.M., 1993. The effect of oxidation on the Verwey transition in magnetite, *Geophys. Res. Lett.,* **20**(16), 1671–1674.

Pal, P.C., Bindu, M.U. & Bhimasankaram, V.L.S., 1971. Early Tertiary geomagnetic polarity reversals in India, *Nature,* **230,** 133–135.

Pande, K., 2002. Age and duration of the Deccan Traps, India: a review of radiometric and paleomagnetic constraints, *Proc. India Acad. Sci.,* **111,** 115–123.

Pande, K., Sheth, H.C. & Bhutani, R., 2001. ^{40}Ar–^{39}Ar age of the St. Mary's Islands volcanics, southern India: record of India–Madagascar break-up on the Indian subcontinent, *Earth planet. Sci. Lett.,* **193**(1-2), 39–46.

Pande, K., Yatheesh, V. & Sheth, H., 2017. ^{40}Ar/^{39}Ar dating of the Mumbai tholeiites and Panvel flexure: intense 62.5 Ma onshore–offshore Deccan magmatism during India-Laxmi Ridge–Seychelles breakup, *Geophys. J. Int.,* **210**(2), 1160–1170.

Pande, K., Pattanayak, S.K., Subbarao, K.V., Navaneethakrishnan, P. & Venkatesan, T.R., 2004. ^{40}Ar/^{39}Ar age of a lava flow from the Bhimashankar Formation, Giravali Ghat, Deccan Traps, *Proc. India Acad. Sci.,* **113,** 755–758.

Patil, S.K. & Arora, B.R., 2003. Paleomagnetic studies on the Dykes of Mumbai region, west coast of Deccan volcanic province: implications on age and span of the Deccan eruptions, *J. Virtual Explor.,* **12,** 107–116.

Patil, S.K. & Rao, D.R.K., 2002. Palaeomagnetic and rock magnetic studies on the dykes of Goa, west coast of Indian Precambrian Shield, *Phys. Earth planet. Inter.,* **133**(1-4), 111–125.

Paul, D.K., Ray, A., Das, B., Patil, S.K. & Biswas, S.K., 2008. Petrology, geochemistry and paleomagnetism of the earliest magmatic rocks of Deccan Volcanic Province, Kutch, Northwest India, *Lithos,* **102**(1-2), 237–259.

Powar, K.B. & Vadetwar, S.V., 1995. Mineralogy and geochemistry of basic dykes and associated plugs of the Revas-Murud Sector, Konkan coastal belt, Maharashtra, in *Dyke Swarm of Peninsular India,* Vol. 33, pp. 1–47, ed. Devaraju, T.C., Mem. Geol. Soc. India.

Prasad, J.N., Patil, S.K., Saraf, P.D., Venkateshwarlu, M. & Rao, D.R.K., 1996. Palaeomagnetism of dyke swarms from the Deccan Volcanic Province of India., *J. Geomagn. Geoelectr.,* **48**(7), 977–991.

Radhakrishnamurty, C., 1993. Magnetic properties of basalts, in *Magnetism and Basalts,* Vol. 20, pp. 158–161, Mem. Geol. Soc. India.

Radhakrishna, T. & Joseph, M., 2012. Geochemistry and paleomagnetism of Late Cretaceous mafic dikes in Kerala, southwest coast of India in relation to large igneous provinces and mantle plumes in the Indian Ocean region, *Bull. geol. Soc. Am.,* **124**(1-2), 240–255.

Radhakrishna, T., Dallmeyer, R.D. & Joseph, M., 1994. Palaeomagnetism and ^{36}Ar^{40}Ar vs ^{39}Ar^{40}Ar isotope correlation ages of dyke swarms in central Kerala, India: tectonic implications, *Earth planet. Sci. Lett.,* **121** (1-2), 213–226.

Ray, R., Sheth, H.C. & Mallik, J., 2007. Structure and emplacement of the Nandurbar–Dhule mafic dyke swarm, Deccan Traps, and the tectonomagmatic evolution of flood basalts, *Bull. Volcanol.,* **69**(5), 537–551.

Rehacek, J., 1994. PMAGIC software for paleomagnetic calculations, Dept. Geol. Washington State Univ., Pullman, Ver. 1.2.

Renne, P.R., Swisher, C.C., Deino, A.L., Karner, D.B., Owens, T. & DePaolo, D.J., 1998. Intercalibration of standards, absolute ages and uncertainties in ^{40}Ar/^{39}Ar dating, *Chem. Geol. (Isotope Geoscience Section),* **145,** 117–152.

Renne, P.R., Sprain, C.J., Richards, M.A., Self, S., Vanderkluysen, L. & Pande, K., 2015. State shift in Deccan volcanism at the Cretaceous-Paleogene boundary, possibly induced by impact, *Science,* **350**(6256), 76–78.

Renne, P.R., Deino, A.L., Hilgen, F.J., Kuiper, K.F., Mark, D.F., Mitchell, W.S., III, Morgan, L.E., Mundil, R. & Smit, J., 2013. Time Scales of Critical Events Around the Cretaceous-Paleogene Boundary, *Science,* **339**(6120), 684–687.

Richards, M.A., Duncan, R.A. & Courtillot, V., 1989. Flood basalts and hot-spot tracks: plume heads and tails, *Science,* **246**(4926), 103–107.

Sahu, R., Kumar, A, Subbarao, K.V., Wlash, J.N. & Biswal, T.K., 2003. Rb-Sr age and Sr isotopic composition of alkaline dykes near Mumbai: further evidence for the Deccan Trap-Reunion plume connection, *J. Geol. Soc. India,* **6**(25), 641–646.

Samant, H., Pundalik, A., D'Souza, J., Sheth, H., Carmo Lobo, K., D'Souza, K. & Patel, V., 2017. Geology of the Elephanta Island fault zone, western Indian rifted margin, and its significance for understanding the Panvel flexure, *J. Earth Syst. Sci,* **126**(1), 9, doi:10.1007/s12040-016-0793-8.

Saunders, A.D., Jones, S.M., Morgan, L.A., Pierce, K.L., Widdowson, M. & Xu, Y.G., 2007. Regional uplift associated with continental large igneous provinces: the roles of mantle plumes and the lithosphere, *Chem. Geol.,* **241**(3-4), 282–318.

Schoene, B., Samperton, K.M., Eddy, M.P., Keller, G., Adatte, T., Bowring, S.A., Khadri, S.F.R. & Gertsch, B., 2015. U-Pb geochronology of the Deccan Traps and relation to the end-Cretaceous mass extinction, *Science,* **347**(6218), 182–184.

Sen, G., 1995. A simple petrologic model for the generation of Deccan Trap magmas, *Int. Geol. Rev.,* **37**(9), 825–850.

Sethna, S.F., 1999. Geology of Mumbai and surrounding areas and its position in the Deccan volcanic stratigraphy, India, *J. Geol. Soc. India,* **53,** 359–365.

Sheth, H.C., 1998. A reappraisal of the coastal Panvel flexure, Deccan Traps, as a listric-fault-controlled reverse drag structure, *Tectonophysics,* **294**(1-2), 143–149.

Sheth, H.C., 1999a. A historical approach to continental flood basalt volcanism: insights into pre-volcanic rifting, sedimentation, and early alkaline magmatism, *Earth planet. Sci. Lett.,* **168**(1-2), 19–26.

Sheth, H.C., 1999b. Flood basalts and large igneous provinces from deep mantle plumes: fact, fiction, and fallacy, *Tectonophysics,* **311**(1-4), 1–29.

Sheth, H.C., 2005. From Deccan to Reunion: no trace of a mantle plume, in *Plates, Plumes, and Paradigms,* Vol. 388, pp. 477–501, eds Foulger, G.R., Natland, J.H., Presnall, D.C. & Anderson, D.L., Geol. Soc. Am.

Sheth, H.C., Zellmer, G.F., Demonterova, E.I., Ivanov, A.V., Kumar, R. & Patel, R.K., 2014. The Deccan tholeiite lavas and dykes of Ghatkopar-Powai area, Mumbai, Panvel flexure zone: geochemistry, stratigraphic status, and tectonic significance, *J. Asian Earth Sci.,* **84,** 69–82.

Storey, M., Mahoney, J.J., Saunders, A.D., Duncan, R.A., Kelley, S.P. & Coffin, M.F., 1995. Timing of Hot Spot–Related Volcanism and the Breakup of Madagascar and India, *Science,* **267**(5199), 852–855.

Subbarao, K.V. & Hooper, P.R., 1988. Reconnaissance map of the Deccan Basalt Group in the Western Ghats, India, in *Deccan Flood Basalts,* Vol. 10, p. 10, ed. Subbarao, K.V., Mem. Geol. Soc. India, (enclosure).

Subbarao, K.V., Ramasubba Reddy, N. & Prasad, C.V.R.K., 1988. Geochemistry and paleomagnetism of dykes from Mandaleshwar region, Deccan Basalt Province, *Mem. Geol. Soc. India,* **10,** 225–233.

Torsvik, T.H. & Van der Voo, R., 2002. Refining Gondwana and Pangea palaeogeography: estimates of Phanerozoic non-dipole (octupole) fields, *Geophys. J. Int.,* **151**(3), 771–794.

Torsvik, T. H., Tucker, R.D., Ashwal, L.D., Carter, L.M., Jamtveit, B., Vidyadharan, K.T. & Venkataramana, P., 2000. Late Cretaceous India-Madagascar fit and timing of break-up related magmatism, *Terra Nova,* **12,** 220–224.

Vandamme, D., Courtillot, V., Besse, J. & Montigny, R., 1991. Paleomagnetism and age determinations of the Deccan Traps (India): Results of a Nagpur-Bombay Traverse and review of earlier work, *Rev. Geophys.,* **29**(2), 159–190.

Vanderkluysen, L., Mahoney, J.J., Hooper, P.R., Sheth, H.C. & Ray, R., 2011. The Feeder System of the Deccan Traps (India): Insights from Dike Geochemistry, *J. Petrol.,* **52**(2), 315–343.

Venkatesan, T.R., Pande, K. & Gopalan, K., 1986. 40Ar-39Ar dating of Deccan basalts, *J. Geol. Soc. India,* **27,** 102–109.

Venkatesan, T.R. & Pande, K., 1996. A review of ^{40}Ar-^{39}Ar Ages from the Western Ghats, Deccan Trap Province, India: implication for K/T events, in *Deccan Basalts,* Vol. 2, pp 321–328, eds Deshmukh, S.S. & Nair, K.K.K., Gond. Geol. Mag.

Verwey, E.J.W., 1939. Electronic conduction of magnetite (Fe_3O_4) and its transition point at low temperatures, *Nature,* **144,** 327–328.

Wensink, H., 1973. Newer paleomagnetic results of the Deccan traps, India, *Tectonophysics,* **17,** 41–59.

Wensink, H., 1987. Comments on "Deccan flood basalts at the Cretaceous/Tertiary boundary?" by V. Courtillot, J. Besse, D. Vandamme, R. Montigny, J.-J. Jaeger and H. Cappetta, *Earth planet. Sci. Lett.,* **85,** 326–328.

Wensink, H. & Klootwijk, C.T., 1971. Paleomagnetism of the Deccan Traps in the Western Ghats near Poona (India), *Tectonophysics,* **11,** 175–190.

West, W.D., 1959. The source of the Deccan Trap flows, *J. Geol. Soc. India,* **1,** 44–52.

West, W.D., 1981. The duration of Deccan Trap volcanicity, *Mem. Geol. Soc. India,* **3,** 277–278.

White, R.S. & McKenzie, D.P., 1995. Mantle plumes and flood basalts, *J. geophys. Res.,* **100,** 17 543–17 585.

Widdowson, M., Pringle, M.S. & Fernandez, O.A., 2000. A post K–T boundary (Early Palaeocene) age for Deccan-type feeder dykes, Goa, India, *J. Petrol.,* **41,** 1177–1194.